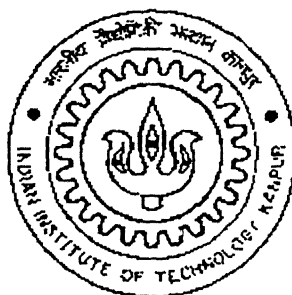# Carrier Mobility and Other Related Measurements in Luminescent Polymeric Thin Film Devices

A thesis submitted
in partial fulfillment of the requirement
for the degree of

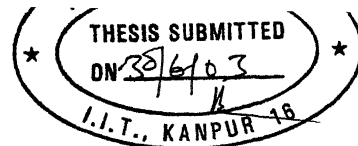## Master of Technology

by

Rahul Dubey

Materials Science Programme
Indian Institute of Technology, Kanpur
June, 2003

CERTIFICATE

It is certified that the work contained in this thesis entitled **"Carrier Mobility and Other Related Measurements in Luminescent Polymeric Thin Film Devices"** by Rahul Dubey has been carried out under my supervision and this work has not been submitted elsewhere for a degree.

(Yashowanta N. Mohapatra)

Professor

Materials Science Programme

Indian Institute of Technology,

Kanpur 208016

June, 2003

i

Acknowledgement

CONTENTS

Abstract

In recent years polymers have proven their potential in fabrication of efficient Polymer Light Emitting Diodes (PLEDs). PLEDs have attracted great interest in the field of large area flat panel displays because of several promising advantages such as bright, efficient, true colour display with large viewing angle, and also ease of processing on large even, flexible substrates. Study of charge transport and mobility of charge carriers is a crucial issue in order to enhance the electroluminescence related performance of such devices. Improvements in transport characteristics can lead to increased device speed, reduced power loss, and avoidance of excessive heating in such promising fields as pixel-resolved full color OLED displays, organic field effect transistor integrated circuits, or photovoltaics. Since in an OLED the light is emitted as a result of recombination of electrons and holes. So balanced charge injection and transport become crucial factors in deciding quantum efficiency of the materials.

In this work the focus was on study of charge transport, specifically mobility measurements in Poly Phenylene-Vinylene (PPV) and its cyno-derivative (CNPPV) polymeric thin film based devices. Devices were fabricated using spin coating of PPV on patterned ITO coated glass substrates. In order to get fairly stable devices fabrication steps were optimized. In addition to conventional sandwich structures, planar structures were also fabricated to carry out current transient experiments.

Current-Voltage characteristics, current transients and elecroluminescence transient experiments were carried out on the fabricated devices. Nature of charge transport and current conduction in two different materials and among different device structures have been compared. Hole current in PPV is found to be space charge limited (SCL) and electron current in CNPPV is found to be dominated by trap filling. However, in case of PPV devices made using two sequential coats of PPV, significant influence of traps on charge carrier transport has been observed. The effect of successive dc biasing sweeps on degradation of characteristics of devices and their slow recovery has been observed. Mobility of the charge carriers is calculated from J-V characteristics and EL transients. Hole mobility in PPV is observed to be 1.0×10^{-5} cm^2/V.sec – 5.0×10^{-5} cm^2/V.sec. The field dependence of mobility is measured and is shown to have Poole – Frenkel (PF) dependence. The parameters associated with P-F dependence compares well with those in the literature. This proves that the PPV material developed at IIT Kanpur is of high quality from the point of view of carrier mobility. In addition to this, in order to probe role of ionic space charge species and polarization in charge transport, current transients have been recorded in planar device structures. There are clear indications that charge transport is affected by presence of a source of internal field due to polarization, ionic space charges or deep traps. Although no quantitative information about the nature of charge transport could be extracted from the current transient experiments with planar structures, we have observed some interesting phenomena related to charge storage and redistribution in PPV and CNPPV base devices.

List of Figures

List of Tables

This thesis deals with characterization of polymer thin film devices to study electrical properties important for Polymer Light Emitting Diode based display applications. In this chapter we give a brief introduction to put the work in perspective.

1. New Class of Polymeric Materials for Photonic Applications:

Initiated by the work of Pope *et. al.* and Heifrich *et. al.* [1,2] on single crystals of anthracene in the early 1960s, photonic applications of molecular and polymeric materials made their way into many fields traditionally dominated by inorganic semiconductors. The potential advantage of organic or polymeric materials is that, thin films of these can easily be made either by vacuum evaporation or by spin coating. In addition to that possibility of manufacturing using inkjet printing technique on polymers is likely to revolutionize large area display and electronic applications. The above mentioned deposition techniques are cheaper and simpler than those used for inorganic semiconductors. Although organic semiconductors possess properties which are advantageous for the integrated circuit industry, they are perhaps best suited to the display industry. Many organic materials have high fluorescence quantum efficiency in the visible spectrum making possible realization of full color displays.

At present there is a strong need to develop a flat panel display, technology alternative to the LCD, motivated by a need to make displays lighter in weight and brighter in colors with a large viewing angle. As for as the OLEDs are concerned, these devices exhibit unique possibilities compared to other exiting display technologies. Organic layers can be deposited on a wide range of substrates including flexible and transparent plastics. This can make possible fabrication of displays which can be rolled. The relative expense of some OLEDs is expected to be so low that greeting cards with messages displayed in OLEDs are a possibility.

In spite of the suitability of polymeric or organic material for large area flat panel displays, there are several drawbacks that hinder the practical application of these devices. One of them is lesser lifetime of these devices as compared to existing displays in market. The lack of understanding of the physics of device operation is also posing a great barrier to their commercialization. However, the development of organic multilayer structures has considerably improved the efficiency of light emission [3,4]. Although in view of poor aging characteristics and low lifetime, the commercial

1

application of OLEDs is restricted at present, there is growing belief in the scientific community that the technology would become commercially viable by innovations based on understanding of charge transport and aging characteristics of these devices.

2. Organic Light Emitting Diodes (OLEDs): A Brief Introduction

These devices, depending upon the material layers used between the electrodes, are referred to either as OLED or PLED. Typically OLED consists of devices fabricated using small molecules and metal chelates, whereas PLED is a specific class of devices using conjugated polymer as functional material.

A typical PLED consists of a single or more than one thin layers of undoped conjugated polymers [5,6] sandwiched between two electrodes on the top of a glass substrate. A single layer diode structure is shown in Fig. 1.1. In this structure the polymer layer is that of PPV. Experimentally attention has been focused on PLEDs that consist a layer of conjugated polymer layer of PPV or its
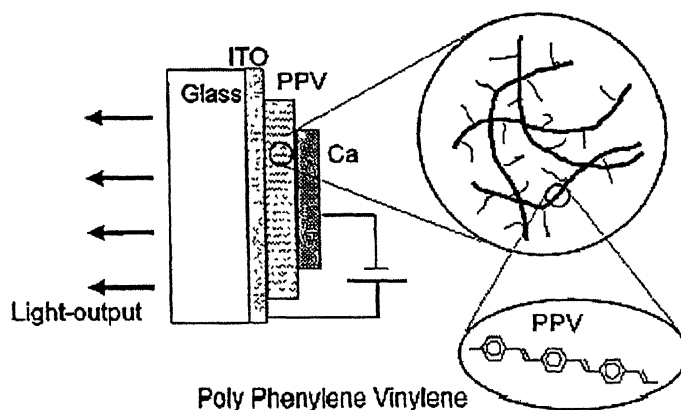
Fig. 1.1 A single layer Polymer LED [7]

derivatives [8]. These materials may have external conversion efficiency larger than 1% photons/charge carrier. The PPV is spin coated on top of a patterned indium-tin oxide (ITO) bottom electrode that forms anode. The cathode on the top of the polymer consists of an evaporated metal layer for which either Ca or Al is used.

The light output or EL is achieved by recombination of positive and negative charge carrier entities. Since in a single polymeric material the charge carrier mobilities may differ by an order or two, which will lead to unbalanced charge transport in a PLED and hence the EL is confined to a region. In case of PPV it has been observed that due to difference in electron and hole mobilities the EL is confined to a region close to the cathode [9,10]. In addition to this there is a larger possibility of presence of pinholes in a single layer of polymer. Thus to improve the efficiency of the device a proper balance of the charge carriers of opposite signs is to be achieved.

The development of multilayer organic structures has considerably improved the efficiency of the light emission by achieving a better balance in number of injected charge carriers of both signs. Also reducing the mismatch of energy levels between the polymer material and the electrode can reduce the operating voltage. Multi layer structures help in design of devices integrating different functionalities. The primary break through in efficiency was achieved in OLEDs by Tang *et. al.* [11,12] by separating functions of electron transport and hole transport to different layers in multiplayer structure. A typical multi-layer structure is shown in Fig. 1.2.
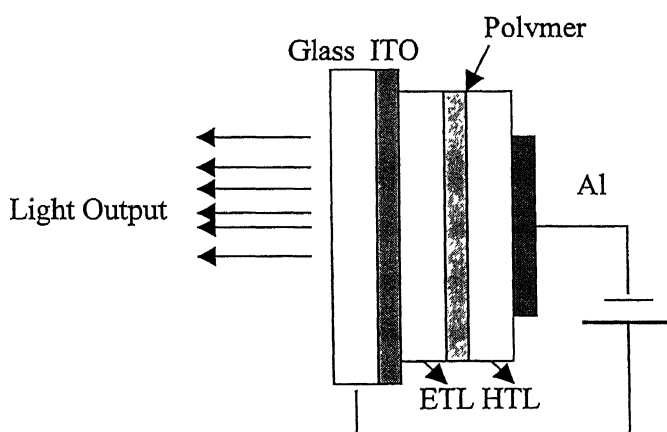
Fig. 1.2 A multi-layer PLED structure. Ideally in a multiplayer structure the active luminescent layer is sandwiched between an electron transport layer (ETL) and a hole transport layer (HTL).

In the multi-layer structure, two or more additional layers may be used. As shown in the Fig. 1.2 the two additional layers ETL and HTL are used. These layers facilitate the movement of electrons and holes in such a way that we get approximately equal number of electrons and holes in the polymer layer. This gives a balanced recombination of the two types of charge entities in the electroluminescent layer improving overall electroluminescence efficiency.

3. Characteristics required for use in a display:

In order to be successful commercially, such an organic light emitting diode (OLED) requires a low driving voltage (< 4V), should possess a high external quantum efficiency (~ 1%), high luminous efficiency (~ 1.5 lm/w) and high brightness (> 1000 cd/m^2). From the fabrication point of view, the polymeric materials should possess easy processibility, which means they can be obtained in form of solutions and can be spin coated on, normally, ITO coated glass substrate. In addition to this, the surface of the polymeric film should be compatible with the electrodes, used for charge carrier junction. The adhesion strength of electrode with polymeric film should be good. In addition to all these requirements we also have to look up for such a material, which is stable against atmospheric degradation and can be processed easily so that their availability is ensured. There is a whole class of materials used by various groups but in this work, studies are restricted to Poly-Phenylene Vinylene (PPV) and it's derivative CN-PPV based devices.

4. Focus of This Work: The Context

In the work presented here, the focus is on charge carrier transport studies in PPV and CNPPV based devices. It includes fabrication of such devices and their characterization to probe into the charge carrier transport, and determination of charge carrier mobilities and their dependence on electric field, which are the key issues in transport studies. The characterization techniques used are current – voltage measurements, slow and fast current transients, and electroluminescence transients.

Understanding of the basic transport mechanisms in this special class of electronic materials is not only of fundamental academic interest, but also bears great technical relevance in that a better understanding may help to increase transport efficiency. This may lead to strategies for increased device speed, reduced power loss and avoid excessive heating in such promising fields as pixel-

resolved full color OLED displays, organic field effect transistor integrated circuits, or photovoltaic cells. In an OLED, among the factors that determine EL device performance, the charge carrier mobilities are significant in two particular regards. The first of those is in relation to the charge balance factor for injection and transport of electrons and holes to the recombination zone. This is a critical parameter in controlling quantum efficiency. Ideally, the electron and hole mobilities should be of comparable magnitude. The second issue is the attainment of the high brightness required for passive matrix addressed displays because there each pixel is turned on for only a fraction of time, and because the eye then time averages this signal, the target peak brightness is in excess of 100 000 cd/m^2. Moreover, in order to ensure acceptable power efficiency this brightness should be reached at low bias voltages. High charge carrier mobilities are essential to achieve such performance level. In addition to that, high mobilities are also essential for the construction of electrically pumped laser diodes [13], efforts towards which are steadily gaining momentum.

The charge transport mechanisms, experimental techniques to determine mobility, and various models explaining field dependence of mobility are more elaborately discussed in chapter 2.

5. Statement of Problem:

This work is devoted to developing experimental facilities and techniques so as to enable characterization of mobility of carriers and electrical properties of materials being developed for PLED application. These measurements provide key feedback to the process of optimizing material and processes being standardized for fabrication of PLEDs at Samtel Centre for Display Technologies at IIT Kanpur. The work, therefore, aims

(1) to develop set-up for mobility measurements by a variety of techniques and device structures,

(2) to determine charge carrier mobility from current-voltage characteristics and electroluminescence transients and their comparison, and

(3) specifically to be use them for determination of mobilities in PPV and PPV-CNPPV structures, and study phenomena related to these measurements in the materials.

1. Device Operation:

Electroluminescence in devices based on organic solids involve following consecutive steps;

  (1) Charge carrier injection,

  (2) Charge carrier transport and

  (3) Radiative recombination of charge carriers.

Fig. 2.1 shows a typical band diagram when HOMO and LUMO levels are treated as bands. Although in these materials there are no such sharply defined bands but we can approximate them as such to understand the production of EL. Anode, which has a work function close to highest occupied molecular orbital (HOMO) level of the organic material, injects holes into the organic layer and cathode, which has a work function close to lowest occupied molecular orbital (LUMO) level of the organic material, injects electrons
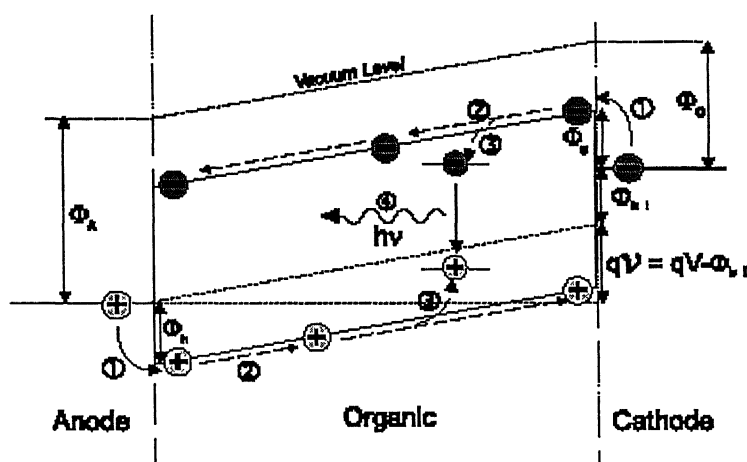
Fig. 2.1: Basic steps of device EL [14]

in organic layer. This is shown in the same figure by means of band diagram. Under the action of applied electric field the holes move towards the cathode and electrons towards the anode. The charge carriers in molecular and polymeric solids carry a cloud of polarization aong with them as they move, and hence they are also referred to as polarons. Further, due to the disorder present in these organic

semiconductors, the mobile charge carriers are readily trapped. Both these mechanisms results in very low charge carrier mobilities, which are the order of 10^{-3} and 10^{-7} cm^2/V.sec [15]. Finally, for electroluminescence (EL), charge carriers of opposite signs recombine to form an exciton, which decays radiatively.

2. Device Physics:

2.1 Charge Transport in Organic Semiconductors:

At first, a summary of the basic concepts, which are responsible for the charge transport mechanisms in case of inorganic and organic semiconductors, is tabulated below. It includes the nature of bonding in two types of materials and formation of filled and vacant energy states based on the nature of bonding.

INORGANIC	*ORGANIC*
■ Strong coupling between atoms	■ Weak intermolecular interactions
■ Delocalisation of electronic states	■ Electronic states are localized
■ Formation of VB & CB	■ Formation of HOMO & LUMO
■ Well explained charge transport	■ Disorder is produced in the form of impurities, cross-links and kinks
■ Phonon assisting tunnelling in case of doped conductors OR Hopping	■ Transport occurs via a sequence of charge transfer steps

The common electronic feature of many organic materials of this area is the π-conjugated system in which σ and π bonds are alternate. The overlapping of pz-orbitals of carbon atom forms such a

system. Due to this overlapping the π-electrons delocalised within a molecule and the energy gap between HOMO and LUMO is relatively small, with transition frequencies lying within the visible region.

PPV
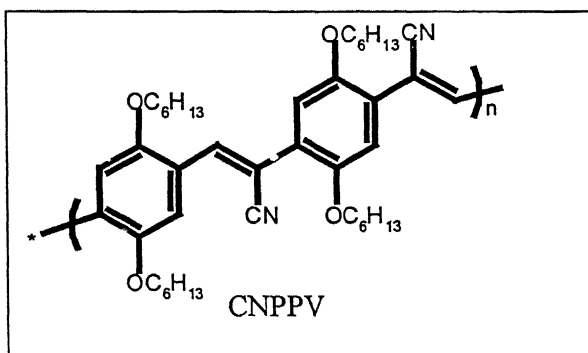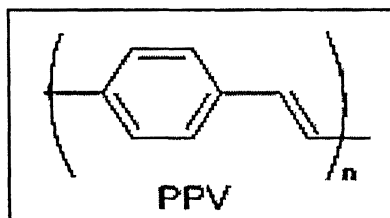
CNPPV

The structures of π-conjugated PPV and CNPPV are shown just above. The low coupling between the molecules in solid state ensures that the carriers in these materials are strongly localized on a molecule. Transport occurs via a sequence of charge transfer steps from one molecule to another, similar to the hopping between defect states in inorganic semiconductors.

2.2 Charge carrier injection and transport:

In organic semiconductors, since the room temperature charge carrier density is negligible, the current conduction in these materials is found to be either injection limited or limited by the bulk of the material itself. Specially, in case of PPV the current-voltage characteristics, current shows bulk limitation or is limited by space charge (SCLC: Space charge limited current). This has been found by

many research groups in a variety of materials [16]. However, for different systems it is not clear which mechanism dominates.

For PPV based LEDs, it has been proven experimentally that hole current is bulk space charge limited, whereas, electron current exhibits trap filled limit (TFL) characteristics [17].

2.3 Space Charge Limited Currents and Trap Filled Limited Currents:

The quadratic dependence of current [18] on applied voltage characterizes the current to be space charge limited, if the experimental data follows the following functional dependence;

$$J = (9/8) \, \varepsilon_0 \varepsilon_r \mu \, (V^2/L^3) \tag{1}$$

where, J is current density, ε_0 is permittivity of free space, ε_r is relative permittivity of polymer, μ is charge carrier mobility, V is applied voltage and L is polymer layer thickness. The above relation assumes that the mobility μ is not dependent on field. Instead, if current is trap limited, the depends of current on voltage is given by means of expression;

$$J = N_c e \mu \, (\varepsilon_0 \varepsilon_r / q N_t)^r \, (V^{r+1}/ L^{2r+1}) C(r) \tag{2}$$

where, $r = T_t / T$, T_t is characteristic temperature for the trap, N_c is effective density of states in the conduction band N_t is total density of traps, C(r) is given by;

$$C(r) = r^r (2r+1)^{r+1} / (r+1)^{r+2} \tag{3}$$

SCLC in the device can occur if at least one contact is able to inject locally higher carrier densities than the material has in thermal equilibrium without injection. The field dependence of current comes usually from the tunnelling of charge carriers. Fowler-Nordheim tunnelling theory predicts [19] predicts that

$$I \propto E^2 \exp(-\kappa / E) \tag{4}$$

Where, I is current, E is electric field strength, and κ is barrier dependent parameter. The tunnelling of charge carriers occurs across a barrier present due to band offset at the polymer and electrode interface. The band diagram, for example, for the ITO/PPV/Al system is shown in the following Fig. 2.2. Here the HOMO and LUMO levels of PPV are respectively 5.1 eV and 2.7 eV. And the work functions of two electrodes ITO and Al are respectively 4.8 eV and 3.1 eV. The respective barriers for holes and electrons are 0.3 eV and 0.4 eV. The hole falls through the barrier in polymer layer at ITO/PPV interface and electrons crosses the barrier hill at Al/PPV interface to enter the polymer layer.

3. Field and temperature dependent mobility in polymeric materials:

From time of flight (TOF) studies, it has been found that charge transport may be dispersive or nondispersive in organic semiconductors [20]. Nature of transport depends upon chemical purity, layer thickness or temperature. The carrier motilities obtained from nondispersive transients reveals basically following features :
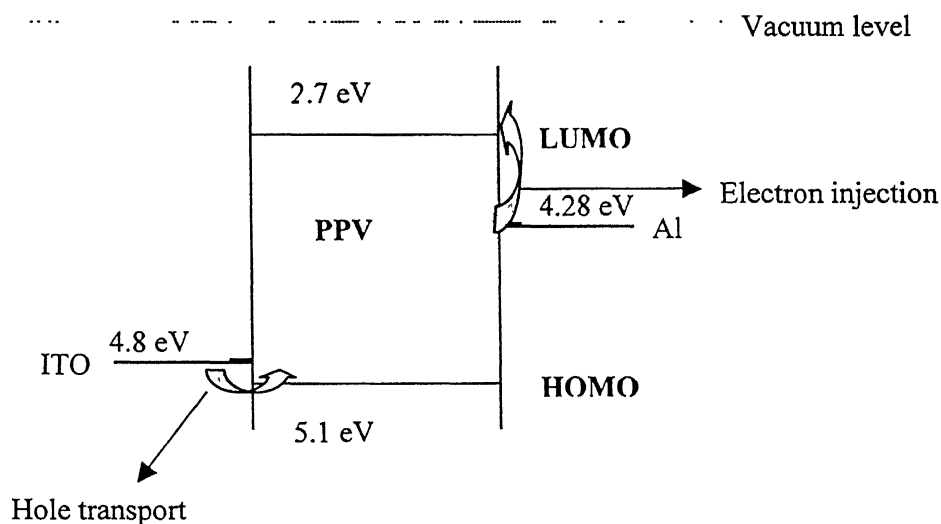
Fig. 2.2 : Band diagram of ITO/PPV/Al device structure

10

(1) a field independent mobility at low fields

(2) a field dependent mobility of the form $\exp(k\,E^{1/2})$

(3) a change of sign for the coefficient k above a certain temperature.

These features can be described by the empirical law proposed by Pai [21] and Gill [22],

$$\mu(E) = \mu_0 \exp\{ -\Delta/k_BT + B(1/\,k_BT - 1/\,k_BT_0)E^{1/2}\} \qquad (5)$$

This phenomenological dependence also applies to hole mobility in PPV based PLEDs [23]. This suggests that the conduction mechanisms in conjugated polymers are similar to molecularly doped systems, where highly localized charge carriers are transported by a thermally assisted intermolecular hopping process. This is assumed to be due to disorder present in the form of kinks, cross-links, and impurities. The conduction depends critically on hopping between conjugated parts of the polymer chain. The equation (5) kind of dependence is well recognized as a modified form of Poole-Frenkel (PF) [24] model of field dependent mobility, and is generally called as PF behaviour. Except PF model there are certain other models such as , Gaussian disorder model (GDM) [25] and correlated disorder model (CDM) [26] which also predict similar dependence. But in all the models the field dependence of PF kind holds either universally or in a particular range of electrical field.

3.1 Poole-Frenkel Model:

Poole-Frenkel field dependence of charge carrier mobility leads to an expression as,

$$\mu \propto \exp(\gamma \sqrt{E}) \qquad (6)$$

According to this model the coulomb potential near a charge localized state is modified by the applied field so as to increase the free carrier density at high fields. By assuming a trap-controlled drift mobility, the Poole-Frenkel model can be applied to drift mobility in polymeric materials. The model would predict an activation energy decreasing as the square root of the applied field. Further, in these polymeric materials such field dependence results from slowly varying spatial fluctuations in he potential energy of a charge migrating through the material. Such energetic fluctuation can arise from [27] a random distribution of molecules in the medium possessing permanent electric dipole moment.

11

Carrier's interaction with these spatial fluctuations provide a significant contribution to the total site energy.

However minimum mobility consistent with a band model is 10^{-1} cm^2/V.sec. Experimental values of μ_0 range from 10^{-4} to 10^{-6} cm^2/V.sec. in polymeric materials implying a higher trap density than the effective density of states in the band. This objection might be removed by the modification of Poole-Frenkel model by Jonscher and Ansari [28], which assumes an energy distribution of localized states through which thermally assisted hopping proceeds. The coulomb potential of much lower density of charged impurity centers are each assumed to extend over many localized states. Thus qualitatively it is expected that these materials exhibit PF kind of behaviour modified to low mobilities due to thermally assisted hopping process.

A second objection to the Poole Frenkel mechanism when applied to the drift mobility is the requirement of for a relatively high density of charged Coulombic centers which in these systems can only be compensated by oppositely charged centers. Ionized centers of this kind are not expected to occur in such organic molecular systems.

In a report by Bagley [29], it is being proposed that the kinetics of localized transport can lead to a activated field dependent drift mobility. The predicted field dependence gives a mobility proportional to $(1/F)$ Sinh($eF\lambda / 2kT$), where λ is separation between the localized states. Another report by Emtage [30] gives the same field dependence by including the effect of an electric field in Holstein's treatment of small polaron motion [31]. Tabak *et al.* [32] have pointed out that this field dependence is far too abrupt to explain the experimental results of field-dependent mobility in amorphous Se, Ae$_2$Se$_3$, and polyvinylcarbazole films.

3.2 Gaussian disorder model (GDM) and correlated disorder model (CDM) :

Bassler and co-workers have extensively studied this model [25]. In this model transport occurs through hopping among the localized states characterized by a Gaussian distribution of site energies. By means of numerical simulation and also being confirmed by experimental results, such a Gaussian density of states leads to a temperature dependence lnμ α $-(T_0/T)^2$. The low temperature transition between dispersive and nondispersive photocurrents is also reproduced by GDM model. However, site energies are distributed independently, with no correlation occurring over any length scale. The field dependence of drift mobility according to the GDM model follows equation (20) for very narrow

range at high fields [33]. Within that narrow range nondispersive mobility is characterized by following expression;

$$\mu = \mu_0 \exp[-(2\bar{\sigma}/3)^2 + C(\bar{\sigma}^2 - \Sigma^2)\sqrt{E}] \tag{7}$$

where, $\bar{\sigma} = \sigma/kT$, is the width of DOS relative to kT and Σ describes spatial disorder, and C is a constant.

In the 1D analysis by Dunlap [34], for a particle moving in a correlated random potential of width σ, mobility is predicted to follow the expression;

$$\mu = \mu_0 \exp[-\bar{\sigma}^2 + 2\bar{\sigma}\sqrt{eaE/kT}] \tag{8}$$

Since 1D transport path is always the same, but in case of 3D it is not fixed, also in this case there is a possibility that the dominant transport path may change with E and T in a way that would alter the essential field dependence. So for 3D case the applicability of equation (21) is doubtful.

In order to get a corrected model for 3D case extensive numerical simulations were carried out on a 3D correlated disorder model (CDM) [35]. Obviously, some of the features of the CDM are similar to that of GDM. However, the Poole-Frenkel dependence of μ is a universal feature of the CDM, independent of the kind of hopping rate, unlike in the case of GDM.

4. Experimental Techniques for Mobility Measurements:

Since in polymeric materials the thermal charge carrier density is negligible so the conventional methods for determination of mobility as Hall-Voltage measurements in case of inorganic semiconductors can not be used for these materials. Some of the techniques, which are used for these materials, are listed below. A brief description of each technique follows the list.

- **Time-of-flight technique**

  transit time carriers generated by UV light pulse/laser pulse;
  $t_T = d^2/\mu V$

- **Transient space-charge limited currents (t-SCLC)**

  transit time of carriers injected from an electrode generated by
  voltage pulse; $t_T = 0.786\ d^2 / \mu\ V$

- **d.c. space-charge limited currents**

  J - V characteristics; by using a proper fitting of J-V characteristics
  in SCL regime; $j = f(\mu, V, d)$

- **Transient electroluminescence**

  delay time of light emission; $t_d = d^2 / (\mu_h + \mu_e)V$

4.1 Time of Flight Technique:

In this experimental method charge carriers are optically generated, using an UV pulse or UV laser pulse ensuring that all the changes are created close to the surface / electrodes. The time taken by the charge carriers to reach at other electrode by drifting can be obtained from the photocurrent transient of the device. This time is called as the transit time (t_T). Since the polymer thickness between two electrodes is known, one can find out the velocity by which charge carriers travel through the material and hence mobility of charge carriers can be determined from the expression; [36]

$$\mu = d^2 / t_T\ V \tag{9}$$

where d is thickness of the polymeric material and V is the applied drifting voltage.

In the experimental set-up the polymer material is sandwiched between two metal electrodes. Light pulse by means of a pulsed laser is produced at ITO side. Thus, charge carries so produced drift towards the other electrode by the applied voltage V across the sample. The transient photocurrent of the device can be recorded across a series resistor R, using a digital oscilloscope. The transit time can be obtained from the photocurrent transient plot. Using this value of transit time one can calculate mobility from eqn. (22). A typical current transient obtained is shown in Fig 2.4 for a PPV sample.
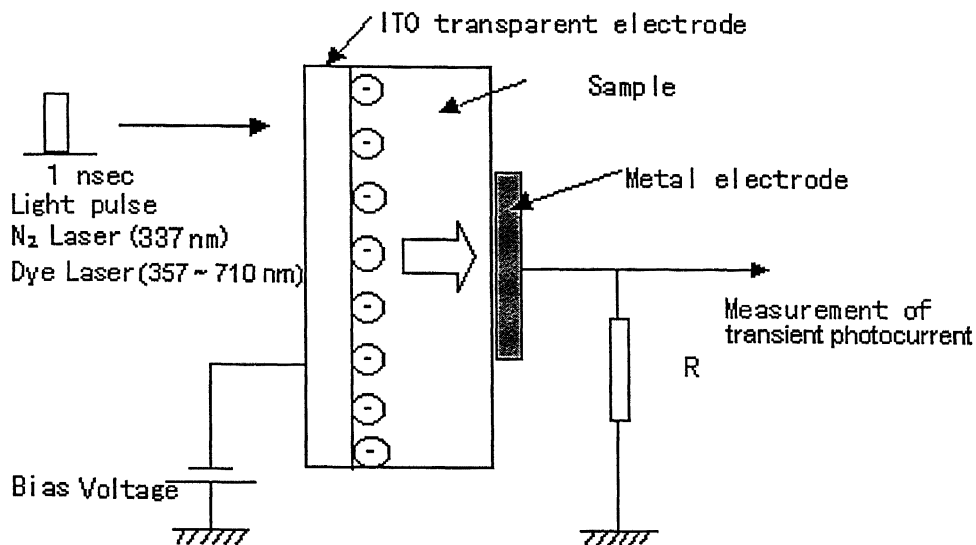
Fig.2.3 : Experimental set-up for TOF measurement
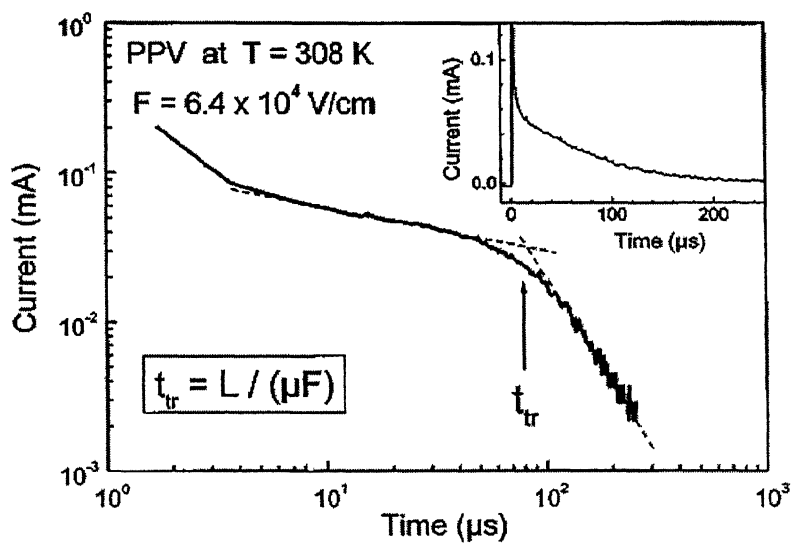
Fig.2.4: A typical TOF photocurrent transient [37].

Some of the limitations of the method are listed below :

Limitations of TOF Technique

(1) With increasing voltage it becomes difficult to distinguish plateau in TOF signal, hence correct determination of t_T becomes difficult.

(2) At low temperatures TOF plateau and falling edge could no longer be achieved.

(3) If charge carriers are trapped then mobility determination by TOF method is not possible. That's why it is not possible to measure TOF signal of electrons in polymeric thin film.

(4) Ensuring that all the light is absorbed near one of the electrons is difficult. To overcome this, many research groups use another thin material layer which serves to generate carriers at the interface. However influence of interface can make interpretation complex.

4.2 Transient Space-Charge Limited Currents Technique:

Based on the theory of transient space charge limited current developed by Many and Rakavy [38], mobility of charge carriers can be calculated. In this experimental method in place of an optical pulse voltage pulse is applied across the device. The device current response as a result of application of voltage pulse is recorded. The peak position of the current gives the transit time. With the help of this transit time, one can calculate mobility using expression;

$$\mu = 0.786 \, d^2 \, / \, t_T \, V \tag{10}$$

where d is thickness of polymer film and V is the applied voltage.

Experimental set-up:
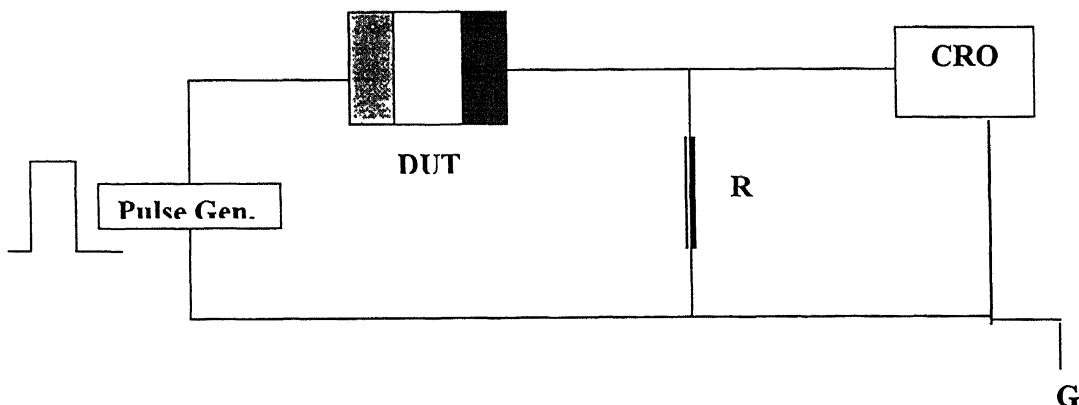
Fig 2.5 : Experimental set-up for recording SCL current transient

16

In this experiment a high input voltage pulse (high enough to drive the device in SCL regime) and of very short duration is given to the device by means of a pulse generator (hp 81101A). The current response of the device across a series resistor R, is recorded by means of a digital oscilloscope (hp 546542B).

Limitations:

To get the current peak, certain conditions have to be satisfied;

(1) An ohmic contact is needed in order to inject the carriers into the polymer material. This requirement (not present in TOF technique) limits this method to materials where an ohmic contact can be made.

(2) Again, similar to TOF technique, if trapping of charge carriers is very strong, the peak can be lost into fast decay of current due to trapping.

(3) One has to make sure that device is biased into space-charge limited region as peak will appear only then.

This technique has recently been used in case of PPV samples[#]. A typical current transient from this experiment is shown in Fig 2.6.
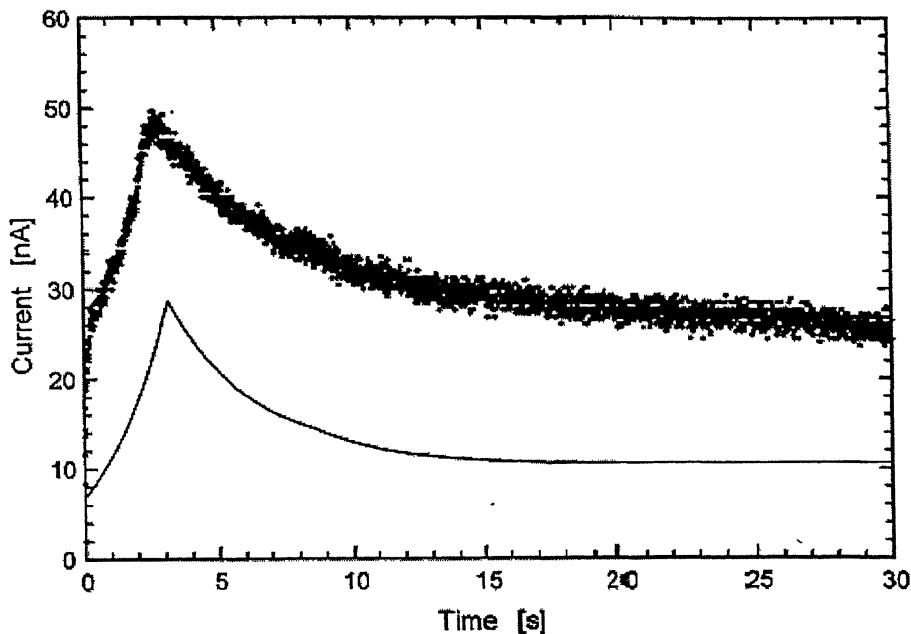
Fig 2.6 : A typical SCL current transient after application of a voltage pulse of height 350V and duration 30 sec across s thin film of thicknes 200 μm.[39]

17

4.3 D.C. Space Charge Limited Currents:

In polymers or organic semiconductors, thermal carriers are generally negligible whereas carriers injected from contacts play a major role. Current becomes limited by the build up of injected space charge and becomes quadratically dependent upon the applied voltage. And the current density can be expressed by means of following expression; [18]

$$J = (9/8) \, \varepsilon \, \mu \, (V^2 / d^3)$$ \hfill (11)

where ε is permittivity of the polymer, d is thickness of polymer layer.

Hence, fitting of experimental J-V plots, using above expression, will lead to calculation of mobility. However this relation is only valid if μ is independent of electric field.

Experimental Set-up:
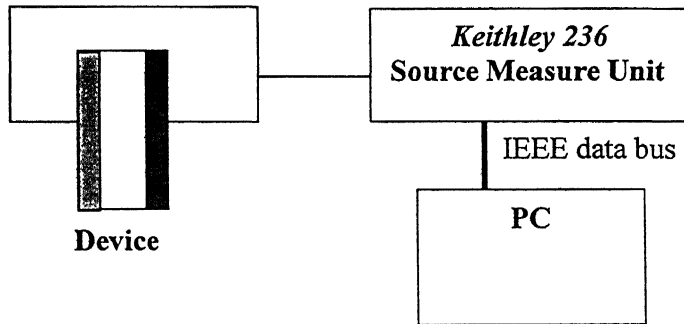
Fig 2.7 : Expt. Set-up for I-V measurement

The d.c. I-V characteristics can be experimentally measured using above experimental set-up, in which voltage in small increments is given to the device and current is measured by the use of a Keithley 236 SMU. The SMU is interfaced with the computer to give data file directly.

18

Limitations:

The non-linear behaviour of I-V can be enhanced by the following factors;

  (1) Presence of traps,

  (2) Field dependence of mobility.

In such cases, it is not possible to find out true relationship of I-V and hence extraction of mobility by fitting the experimental data by means of expression (3) will not give correct values.

4.4 Field Dependent Mobility from SCL I-V; Differential Method:

This method has been proposed recently by Natali [40]. It proposes charge carrier mobility determination of mono charge carrier space charge limited devices. It is a general method and mobility can be extracted independently from I-V data without knowing the exact dependence of mobility on field. Since the quadratic behaviour of SCL currents [41] in these devices may not be obtained and it may show even a higher degree of nonlinearity due to presence of trapping states or field dependent mobility. In such cases an explicit current voltage relation cannot always be found. This method promises to be helpful in extracting mobility from I-V data only. Natali has worked out an expression for field dependent mobility in case of trap free and space charge limited regime;

$$\mu(\mathcal{E}_c) = \frac{L^3}{\epsilon} \frac{J}{V^2} \left(\frac{p^2}{p+1} \frac{1}{1 + \frac{1}{p} - \frac{1}{p} \frac{d \ln p}{d \ln V}} \right) \qquad (12)$$

where, L is thickness of polymeric film, p is slope of I-V curve on a log-log scale, and E_c is electric field at collecting electrode. There are no reported experimental results on this technique. In this work we use this method to obtain mobility.

4.5 Frequency Dependent Mobility from Admittance Spectroscopy:

As discussed in sections, given above hole mobilities in conjugated polymers can extensively be studied from (1) TOF or (2) J-V characteristics. But investigation of electron transport has not yet been possible. Thus, to improve the present knowledge of carrier transport in PLEDs requires a

technique capable of deriving both electron and hole transport. The technique presented by Martens *et.al.* [42,43] is based on use of admittance spectroscopy on PLEDs. Charge transport at time scale τ is reflected into frequency domain around ω ~ τ^{-1}, can give information about different dynamical processes. Finite transit time τ_t holes in PPV based hole only devices is reflected in the admittance. From specific frequency dependent response the hole mobility could be derived. In the PLED the transit of both electron and hole can be clearly separated in the frequency domain, giving the respective mobilities. In contrast to J-V and TOF, admittance spectroscopy does not suffer from the presence of deep traps, since release rates from deep traps are << $1s^{-1}$ and, hence, falls out of the frequency range (Hz to MHz), studied in admittance spectroscopy. Under the influence of the ac electrical signal, the admittance Y is complex and given by,

$$Y = i_{ac}/v_{ac} = G + i\omega C$$

Where, G is conductance and C is capacitance. The inductive contribution (i.e., negative capacitance effects) under application of bias is observed. If C_0 be the geometrical capacitance then to see the inductive contribution more clearly differential susceptance $-\Delta B(\omega) = -\omega (C-C_0)$ is plotted as a function of frequency, see Fig. 2.8.
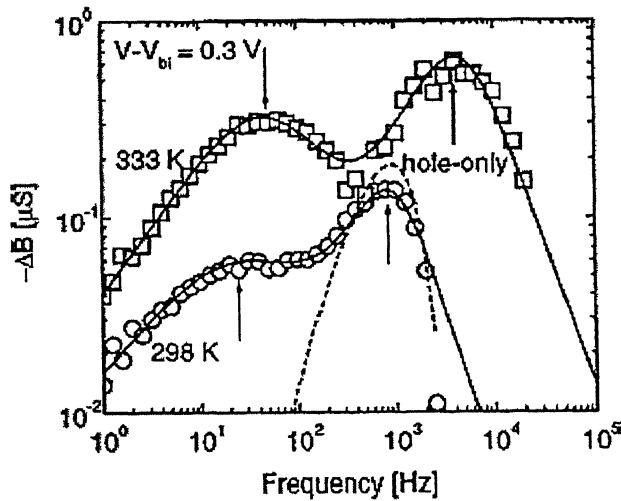
Fig.2.8 : Double logarithmic plot of negative susceptance of a PLED[30]

20

The inductive contribution in hole only devices stems from redistribution of space charge when the electric field is varied. Changing the applied voltage leads to injection of additional space charge. Under the influence of the bias field, the injected charge moves into the device to relax to the new equilibrium space charge distribution of. Due to the finite transit time τ_t the corresponding current lags behind the ac voltage, and this gives an inductive contribution to the capacitance. The peak corresponds to hole transit peak and it can give τ_p, from which hole mobility can be derived.

4.6 Transient Electroluminescence Technique:

This method is based on the presence of time lag in EL on application of a voltage pulse [44,45] In this experimental method one has to measure the delayed electroluminescence. After a voltage pulse is applied to the device. Injected holes have to flow to the cathode before light generation occurs. Thus, observed time lag is directly related to transit time of holes towards the cathode. The equivalence of transit time obtained from the delayed electroluminescence and from the TOF technique has been confirmed experimentally. In case of non-dispersive transport the hole transit time, t_T then directly provides information about the hole mobility according to expression;

$$\mu = d^2 / t_T (V - V_{bi})$$ (13)

where V_{bi} is built in voltage and d is thickness of polymer film.
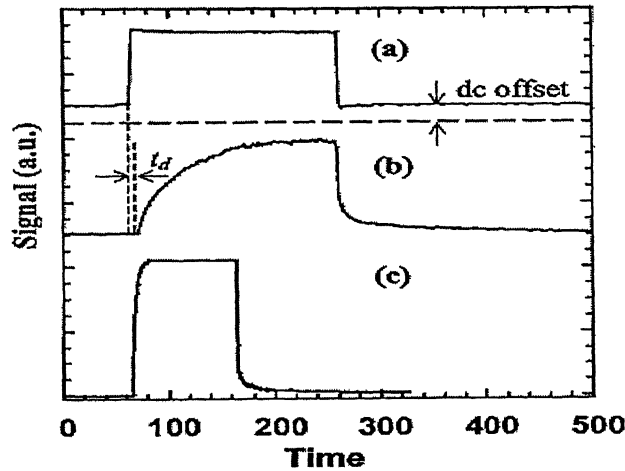
Fig 2.9 : (a) Input pulse applied to the device, (b) EL response at low voltages
(c) EL response at high voltages [46]

In this experimental technique, input voltage pulse is applied by means of a pulse generator and observed EL is recorded in the form of out-put current of the PMT by a digital oscilloscope. The time lag between the application of voltage pulse and onset of EL is the required transit time t_T. Also a typical EL transient is shown in Fig. 2.9.

5. Typical Mobility Results: A Comparison

In the present work, our focus is on charge carrier transport in PPV and CNPPV thin films as a measure of electrical quality of materials being developed, and validation of process steps used to fabricate devices. In the Table 2.1, mobility of holes/electrons in PPV obtained by different methods, discussed above and with critical remark is listed. Table 2.2 shows mobility measurement results and corresponding experimental techniques, in other related materials. From these results, it can be concluded that in these materials mobility ranges from 10^{-7} cm^2/V.sec to 10^{-3} cm^2/V.sec. Especially in case of PPV mobility is around 10^{-5} cm^2/V.sec, with a field dependence of PF kind.

Material	Method	Results	Remarks	Ref.
MEH PPV	TOF	9.8×10^{-6} cm2/Vsec after annealing 4.5×10^{-7} cm^2/V sec → both are hole mobilities.	Nondispersive hole transport does not exist after annealing because of formation of nano scale domains, which enhances inhomogeinity.	47
PAPPV	TOF	$\sim 10^{-4}$ to 7×10^{-3} cm^2/Vsec	Mobilities obtained from TOF The higher mobility of copolymer is due to its more ordered structure. Mobility shows a PF kind of field dependence.	20
MeL PPP	TOF	$\sim 10^{-4}$ to 7×10^{-3} cm^2/Vsec		
bis - flourene	TOF	$\mu_h \sim 2.0 \times 10^{-4}$ cm^2/Vsec	TOF mobility shows a very weak field dependence as mobility increases from 2.0×10^{-4} cm^2/Vsec at ($E \approx 0.2 \times 10^6$ V/cm) to 3.0×10^{-4} cm^2/Vsec at ($E \approx 0.2 \times 10^6$ V/cm) only.	48

Table (2.2) : List of experimental mobility values from different methods in different materials

Alq	TOF	$\mu_e \approx 10^{-6}$ cm^2/Vsec	Mobility exhibits strong field dependence according to Poole-Frenkel form	49
DPOP-PPV	TOF	$\mu_h \approx 2 \times 10^{-4}$ cm^2/Vsec	----------	23
PDAOPV	J-V	$\mu_h \approx 5 \times 10^{-7}$ cm^2/Vsec	----------	3
PPPV	TOF	$\mu_h \approx 5 \times 10^{-5}$ cm^2/Vsec	----------	50
PFO	TOF	$\mu_h \approx 4 \times 10^{-4}$ cm^2/Vsec	TOF signsl shows dispersive transport, with mobility showing field dependence of PF kind.	51

Table (2.2) : List of experimental mobility values from different methods in different materials, contd…

Experimental Mobility Values in PPV based PLEDs from different experimental techniques:

Material	Technique	Mobility	Comment	Ref
PPV	Delayed EL	$\mu_h \approx 10^{-5}$ cm^2/Vsec	Response of LED under pulsed operation is dominated by the dispersive transport of holes towards the cathode.	52
PPV	TOF	$\mu_h \approx 10^{-5}$ cm^2/Vsec	Mobility depends on electric field according to Poole-Frenkel model ; $\mu = \mu_o \exp(\sqrt{E/E_o})$	53
PPV	J-V	$\mu_h \approx 5 \times 10^{-5}$ cm^2/Vsec	The hole transport is well described by space charge limited current	3
PPV	SCL Current Transient	$\mu_h \approx 4.2 \times 10^{-7}$ cm^2/V sec	This is almost field indepen-dent mobility since fields are too low to demonstrate field dependence of mobility; and the value close to that obtained by TOF technique at room temperature.	26
PPV	TOF	$\mu_h \approx 1.4 \times 10^{-5}$ cm^2/V sec	Mobility depends on electric field according to Poole-Frenkel	54
PPV	SCLCT	$\mu_h \approx 4.5 \times 10^{-5}$ cm^2/V sec	Mobility depends on electric field according to Poole-Frenkel	54

Table (2.2) : List of experimental mobility values from different methods in PPV

25

In order to study charge carrier transport, different kinds of samples using thin films of polymers PPV and CNPPV have been fabricated. A detailed list of kinds of samples is given in Table 3.1. In this chapter, all the fabrication steps and experimental setups are discussed in detail.

1 Fabrication of devices:

Steps involved in fabricating a complete device are summarized in the block diagram given in Fig. 3.1. However, each step is being discussed in detail under this section. To make a device , one has to start with ITO sputtered glass substrates, which are usually available in a size of 2x2 inches. The same can be cut to an appropriate dimension using a diamond cutter.

1.1 Step (I): Cleaning of ITO coated glass substrates or plane glass substrate:

The standardized cleaning procedure for such substrates is described below:

(1) **RCA Cleaning:** At first substrates are cleaned in the chemical solution ammonium hydroxide (NH_4OH), deionized water ($DI-H_2O$) and hydrogen peroxide (H_2O_2), at a temperature of $80 - 90^0C$, at least for duration of 10 minute. This cleaning is popularly known as RCA cleaning. The ratios of different solutions are:

NH_4OH	H_2O_2	$DI-H_2O$
1	1	5

After RCA cleaning substrates are rinsed in DI-water at room temperature.

(2) **Ultrasonic Cleaning:** RCA cleaned substrates are further kept in an ultrasonic cleaner for 5 minutes. The medium used for cleaning is di-water.

After ultrasonic cleaning substrates, are dried by a hand drier.

(3) **Heating of substrates:** Cleaned and dried samples are heated in on oven at a temperature of 120^0C for 1 hour. Heating is done to remove any moisture from the substrate.

26
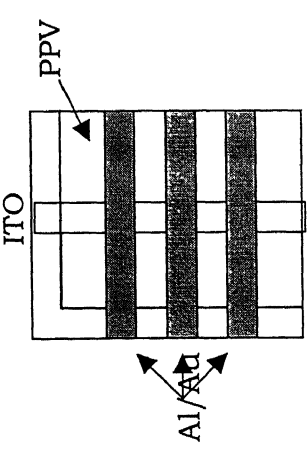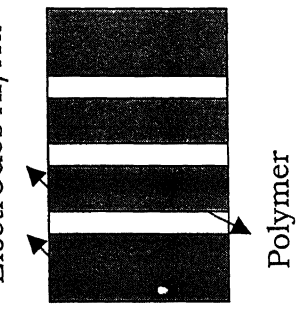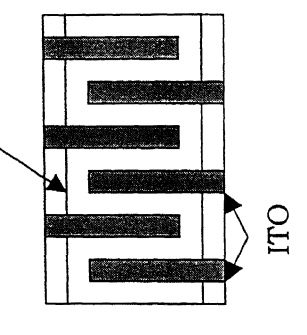
Devices			
Sandwich- Structure		**Planar- Structure**	
Double charge carriers	Monocharge carriers	Hole transporting	Electron transporting
ITO/PPV/Al ITO/CNPPV/Al	ITO/PPV/Au (Hole transporting) Al/CNPPV/Al (Electron transporting)	ITO/PPV/ITO Au/PPV/Au	Al/CNPPV/Al
Structures used:			

Table 3.1 : Detailed list of devices, fabricated for this work

27

1.2 Step (II): Patterning of ITO using photolithography:

If glass substrate is coated with indium tin oxide (ITO), which acts as a anode in the device. Sputtered ITO has to be patterned according the design of the devices on a substrate. Patterning can be done using photolithography, which involves following steps,

(1) **Substrates:** Cleaned ITO coated glass substrates are preheated for 30 minutes at 120^0C temperature in order to remove any moisture from it.

(2) **Coating of photo resist:** Thick photo resist is spin coated at 1000 RPM with one-minute time of spinning.

(3) **Pre-baking:** Pre-baking of ITO substrate, coated with photo resist is done in oven at 85^0C for 20 minutes.

(4) **Exposure to UV light:** UV light is exposed on the pre-baked samples, while covering the samples with appropriate pattern in the form of a mask. The time of exposure is usually 3 minutes. The area, which is exposed to UV light, is hardened and rest of it is left soft.

(5) **Developing:** After exposure to UV light samples were developed using PF developer for 1.5 minutes and then rinsing them in solution of n-butyl acetate for 1.5 minutes. In the process of developing the soft portion of photo resist layer over substrate is removed, whereas hardened photo resist layer remains.

(6) **Post-baking:** After developing, the samples are kept in oven for 20 minutes at temperature 135^0C. This step is called as post-baking. This is done to harden the photo resist further so that under that ITO layer remains protected during etching process.

(7) **Etching:** Etching is the process, which removes ITO from the glass substrates. An etchant is a mixture of di-water, hydrochloric acid (HCl) and nitric acid (HNO_3) in proper ratio. Samples are kept in etching solution for 4 to 5 minutes and a temperature of 50-55^0C is maintained. During etching all ITO except where it is being covered by hardened photo resist layer is removed. The respective ratio of three constituents of etching solution are,

di-water	HCl	HNO_3
150 ml.	40 ml.	10 ml.

```
┌─────────────────────────────┐
│  Cleaning of ITO coated glass│
│           substrate         │
└─────────────────────────────┘
                │
                ▼
┌─────────────────────────────┐
│  Coating of photoresist on the│
│           substrate         │
└─────────────────────────────┘
                │
                ▼
┌─────────────────────────────┐
│  Exposing to UV light with  │
│     appropriate mask        │
└─────────────────────────────┘
                │
                ▼
┌─────────────────────────────┐
│  Development of photo -     │
│    resistive polymer        │
└─────────────────────────────┘
                │
                ▼
┌─────────────────────────────┐
│  Etching of ITO to create   │
│    appropriate pattern      │
└─────────────────────────────┘
                │
                ▼
┌─────────────────────────────┐
│  Stripping of photoresistive│
│           layer             │
└─────────────────────────────┘
                │
                ▼
┌─────────────────────────────┐
│  Coating of polymer thin    │
│           films             │
└─────────────────────────────┘
                │
                ▼
┌─────────────────────────────┐
│  Metallization of cathode   │
│  using suitable             │
│  mask                       │
└─────────────────────────────┘
```
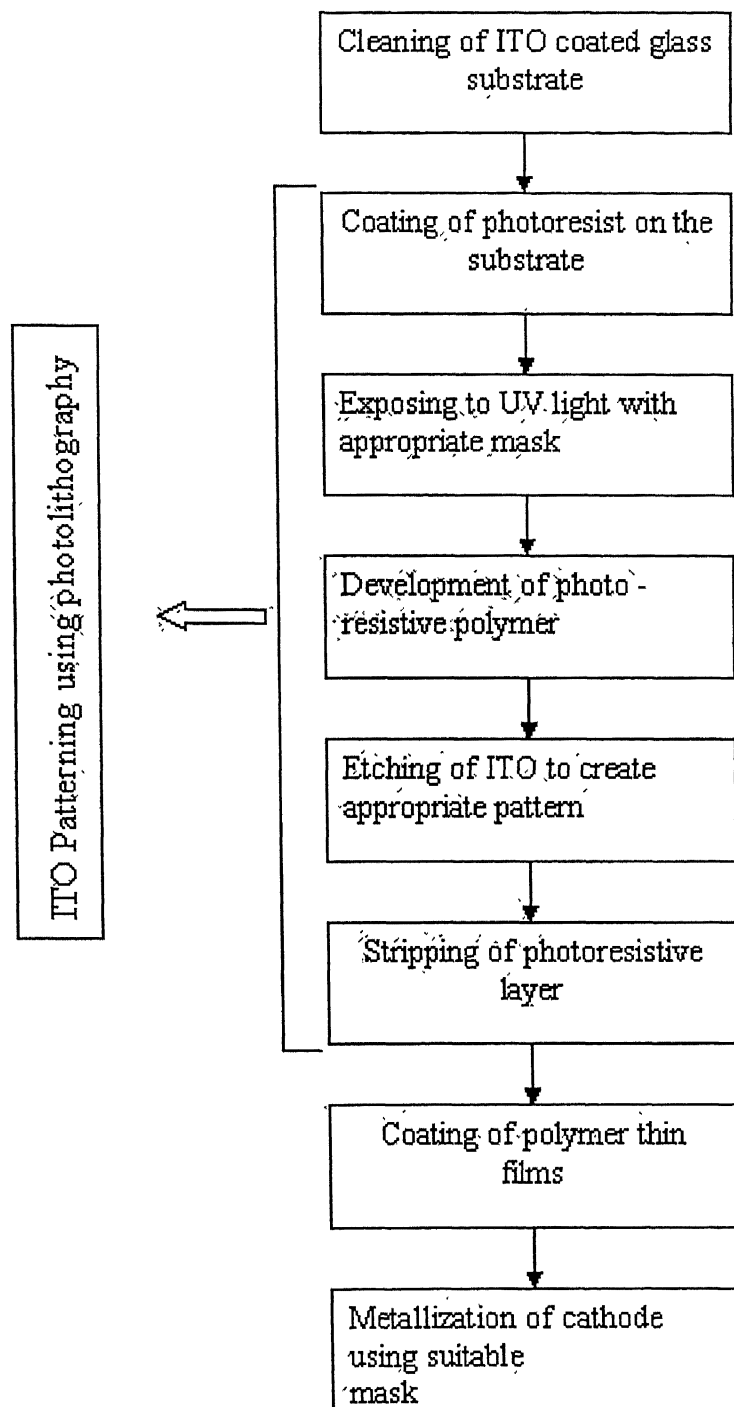
ITO Patterning using photolithography ⇐

Fig. 3.1: Block diagram of fabrication steps

29

(8) **Stripping:** This step removes the photo resist layer from the substrate and thus exposes the ITO under that. The etched samples are dipped in stripping solutions, in each of the two for one minute and at a temperature of 90^0C.

After stripping is over, patterned ITO substrates are rinsed in hot water and then cleaned using RCA cleaning followed by ultrasonic cleaning. After that substrates are dried with a hand drier. Now these substrates are ready for deposition of polymer films.

1.3 Step: (III) Coating of PPV thin film on substrates:

PPV itself does not dissolve in most solvents. Hence spin-coating is done using a solute precursor. PPV precursor prepared by Xanthate process is dissolved in cyclohexane and solution is prepared by magnetic steering and centrifuging. To take it in the form of solution is essential so that it can be spun onto the substrate. The coating of thin films is carried out in following steps:

(1) **Pre-heating:** ITO patterned and cleaned glass substrates (also plan glass substrates) are kept in oven for 30 minutes at a temperature of 160^0C. Pre-heating is done to remove any kind of moisture present on it.

(2) **Ozonization:** During various cleaning processes the work function may change due to chemical reactions at ITO surface. This step is crucial in order to recover work function of ITO, since work function of ITO controls the injection of holes and hence the device performance. In this process, pre-heated substrates are kept in ozonozation chamber for 7 minutes. Oxygen is passed in the chamber where it converts into ozone under the action of UV light.

(3) **Spin coating:** PPV precursor solution of concentration 18mg/ml is spun on the ozonized substrates at 1000 rpm, for one minute. If a double coat of polymer is required then polymer-coated samples are kept in oven for 10 minutes at 160^0C temperature. After taking out the sample a second layer is spun on that, with same spinning parameters.

(4) **Vacuum drying:** After spin coating, substrates are placed in a vacuum chamber, where they are heated at 120^0C temperature for 2 hours. During heating vacuum level of 10^{-5} mbar is maintained. This heating evaporates the solvent (cyclohexane) from thin film of polymer.

(5) **Thermal conversion:** Vacuum dried samples are kept in oven, so that PPV precursor is converted into polymer. This thermal conversion is carried out at 180-185^{0}C temperature for 6 hours, under the N_2+H_2 ambient.

Thermally converted polymer thin films, onto the substrates are ready for cathode deposition. Deposition of cathode can be made using Physical Vapor Deposition method.

1.4 Step (IV): Cathode deposition:

Top metal electrode films are deposited by vacuum coating of metal, using vacuum coating unit. All the steps involved in operating a vacuum coating unit are given here.

(1) **Loading:** At first vacuum chamber is thoroughly cleaned. PPV deposited samples are kept above the mask. Metal, to be deposited is loaded in the tungsten filament. Then chamber is closed and air admittance valve to the chamber is closed properly.

(2) **Roughing:** Rotary pump (RP) is switched on. The vacuum valve (not the high vacuum valve) is turned to position roughing. During roughing the vacuum chamber is evacuated.

(3) **Backing:** When vacuum level in the chamber drops down to 0.02-0.01 m.bar (as red by the pirani gauge of the coating unit). The vacuum valve is turned to position backing. During backing the pipelines connecting Diffusion pump (DP) to vacuum chamber, are evacuated.

(4) **Creating high vacuum:** When vacuum level during backing reaches to 10^{-3} m.bar, switch on the diffusion pump (DP). One has to wait for 20-25 minutes and then open the high vacuum valve and start reading vacuum level in pen-ing gauge.

(5) **Coating of metal electrode:** When the vacuum level reached 10-6, metal is fired by supplying current to heating filament. The vapor of metal is deposited on the polymer-coated substrates through masking.

Finally metal electrode deposited samples are taken out of the vacuum chamber. Thus devices are ready for measurements.

2 Experimental Setup and Measurements:

This work involves current measurements as a function of voltage and time, in vacuum. Along with d.c.current-voltage characteristics and current transient measurements, Impedance and EL transient measurements were also carried out using different experimental setup.

2.1 Cryostat and Measurements in Vacuum:

These polymeric materials, under electrical biasing are very sensitive to degradation due to reaction with oxygen and moisture present in atmosphere. So in order to prevent degradation measurements have to be carried out in vacuum. For this purpose a cryostat with a provision of cooling and heating arrangements has been designed. Inside the chamber vacuum of the order of 10^{-3} can be created by means of a rotary pump. The design of cryostat is given in Fig.3.2. The device is mounted on a sample holder made of copper with electrical connections made on a L shaped PBC plate. External connections from outside are taken from the BNC connector port. If cooling of the sample is desired, it can be achieved by dipping copper rod in liquid nitrogen and temperature of the sample can be read by the means of a thermocouple, provided for the purpose, in this design. In addition to that, in order to carryout some measurements requiring photo excitation, quartz glass windows can be put in the window cover of upper part of the chamber.

2.2 Current vs. Voltage Measurement:

IV measurements are carried out using Keithley 236 (Source Measure Unit), which directly reads the current values and supplies voltage as per the instructions given by the programme. All the parameters, like voltage limits, time of measurements, and voltage steps can be controlled by computer. The sample is mounted inside the cryostat and connections are taken from the external connecting ports, through BNC connectors. The experimental setup is given in Fig.3.3. The same experimental set up can also be used for long time current transient (msec. to sec.) measurements, open circuit voltage measurement and short circuit current measurement. All the different measurements are computer controlled.

2.3 Pulsed Current Transient Measurement:

For short time current transient (in micro sec.) measurements, an electrical pulse of very short duration is applied to the device by a HP 81101A (50 MHz) Pulse Generator. The device current is recorded by a HP 54615B (500 MHz) digital storage oscilloscope, which is interfaced to computer through RS232 data bus. Thus, data and waveform can be captured for further analysis. The experimental setup, used for these measurements is given in Fig.2.5 in chapter 2.
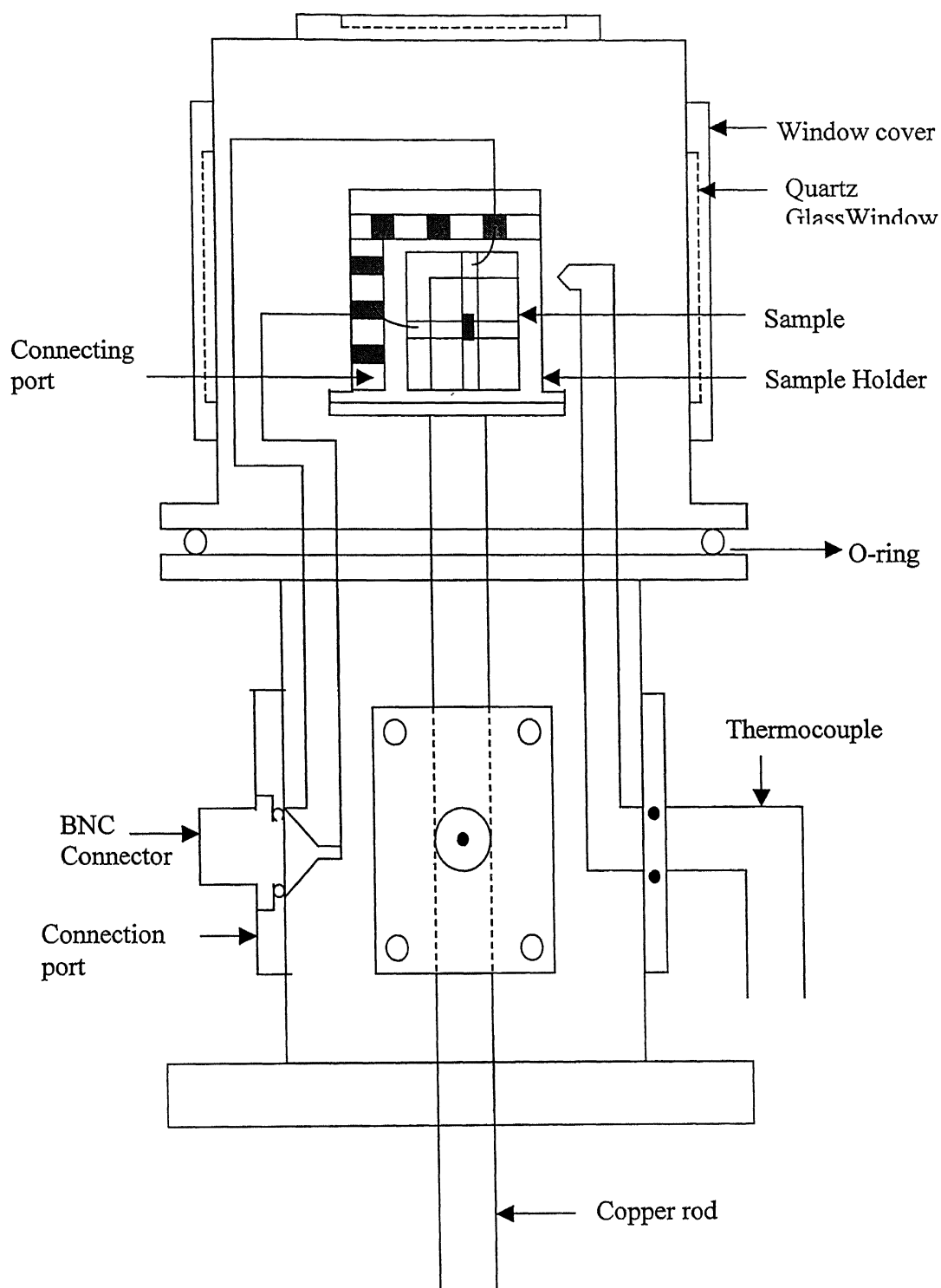
Fig. 3.2: Design of home made cryostat
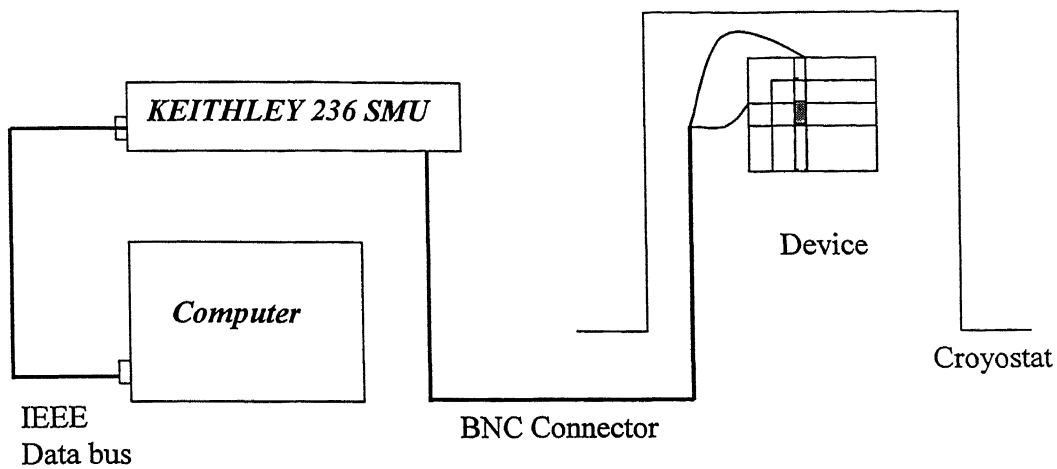
Fig.3.3: Setup for I-V measurement in vacuum

2.4 Electroluminescence Transient Measurement:

For EL transient measurement, the experimental setup is given in Fig. 3.4. A voltage pulse of a short duration is applied to the luminescent device by the same pulse generator as discussed in above heading. This pulse generator can produce pulses upto a duration of a few hundred nanoseconds. The device is mounted below a PMT that can pick up EL response of device. The input of pulse from the pulse generator and output signal from PMT are recorded on the digital storage oscilloscope. Thus time delay in EL can be measured by comparing the time scales of input and output voltage pulses.

2.5 Impedance and Capacitance vs. Voltage Measurement:

The experimental setup for impedance measurement is shown in Fig. 3.5. Impedance measurements were done using a SR830 DSP Lock-in Amplifier. In this measurement an a.c. reference signal along with a d.c. bias is given to the sample, mounted in cryostat, by means of a adder circuit. The frequency is varied over a large range in order to see device response. The lock-in amplifier, interfaced to computer through a GPIB interface card, records the sample response in the form of current amplitude

34

and phase angle. Same setup can be used for capacitance vs. voltage measurement, in which frequency is kept constant and bias is changed and output current amplitude, phase angle is used to compute device capacitance.

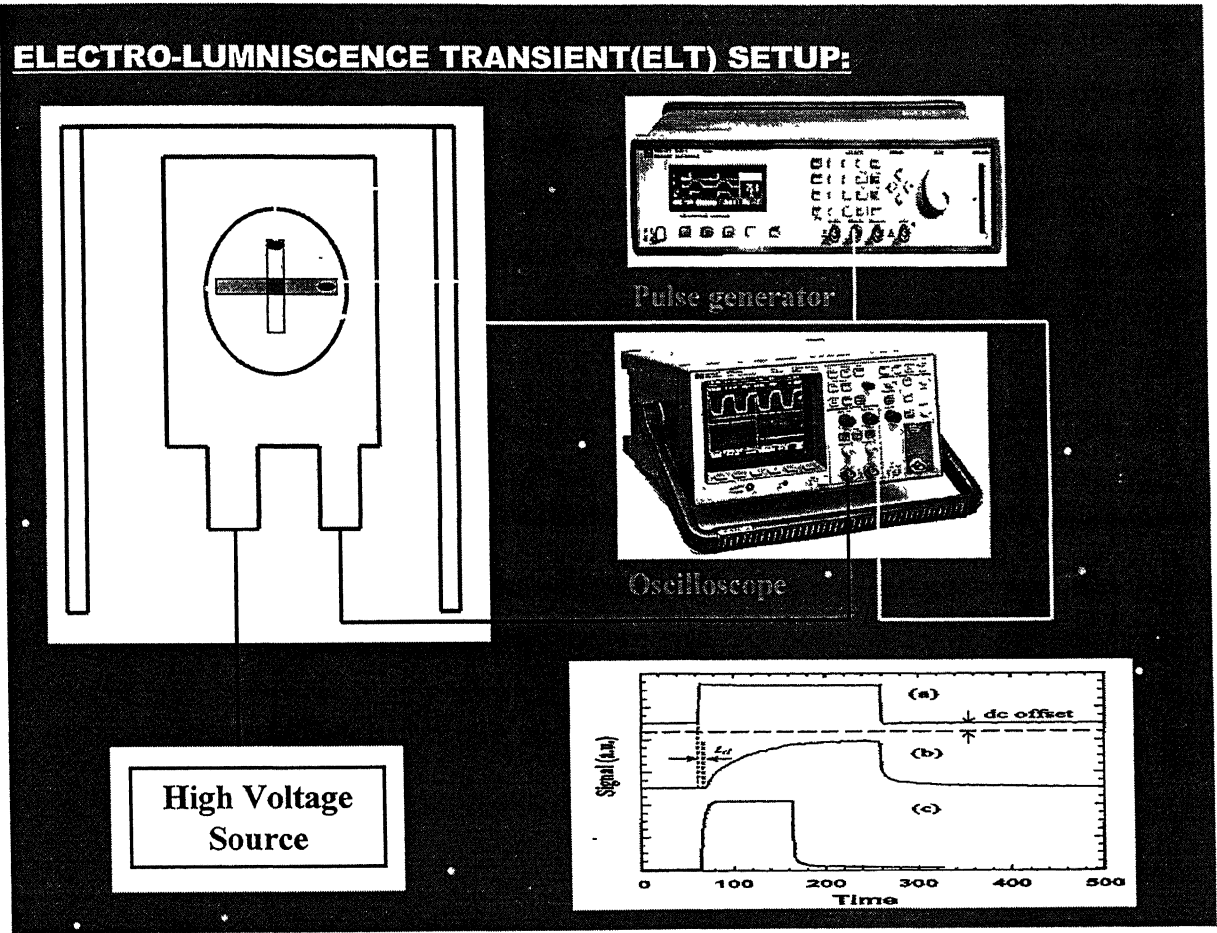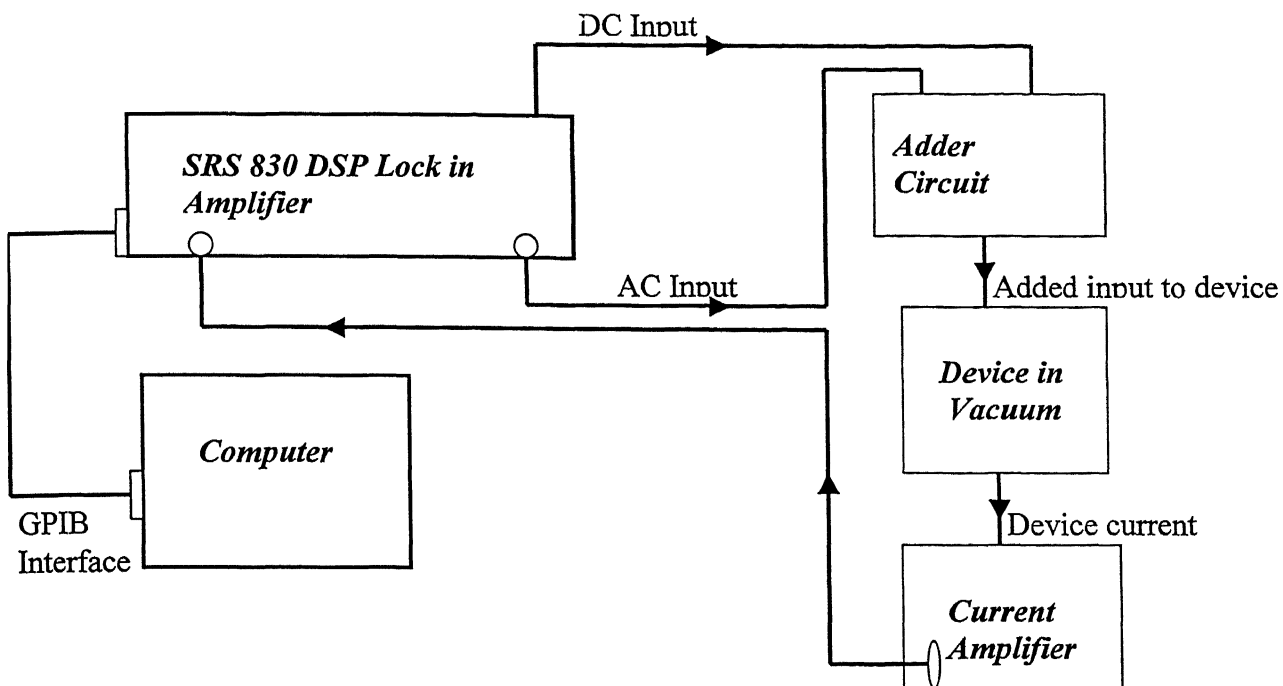Fig.3.4: Experimental set-up for obtaining transit time from delayed EL

Fig.3.5: Setup for Impedance and C-V measurement

This chapter is organized into three distinct parts. We first discuss forward I-V characteristics various structures. These measurements are basic to any conclusions regarding transport properties Then we go on to determination of mobility by I-V and electroluminescence transient methods. In t last part we take up various interesting electrical phenomena that we observed during our attempts make mobility measurements such as current transients, and sweep dependent I-V characteristics. Tv types of structures have been used in this study as described in chapter 3 already. The sandwich across structures are directly relevant to devices being developed for PLED applications. Plan structures were designed to attempt mobility determination in simple electrical pulsing experimen and to compare possible difference in mobility as measured at the top of the film and near the interfa at the substrate. We succeeded in measuring mobility in sandwich structures. Though our attempt make mobility measurements in planar devicesdid not succeeds, it did provided interesting insights f future work.

In order to study transport of different types of charge carriers (electrons and holes), t structures of devices used for studies are given below:

[a] Sandwich or Across Structures:

    (1) ITO/PPV/Au : hole only device.

    (2) Al/CNPPV/Al : electron only device.

    (3) ITO/PPV/Al : dual charge carrier devices.

    (4) ITO/CNPPV/Al : dual charge carrier devices.

    (5) ITO/PPV/CNPPV/Al : dual charge carrier, double layer devices.

[b] Planar Structures:

    (1) ITO/PPV/ITO : hole only device.

    (2) Au/PPV/Au : hole only device.

    (3) Al/CNPPV/Al: electron only device.

Band diagrams of these device structures are given in Fig. 4.1 and 4.2. The common feature is tha the work function of electrode lies closer to HOMO level of polymer, it will inject holes and if it l

closer to LUMO level, it will inject electrons. Experimental results for different device structures a organized in such a way that a possible explanation is given after the description of the feature obtained in results. Also a comparison among different kinds of devices is appended to tl explanation.

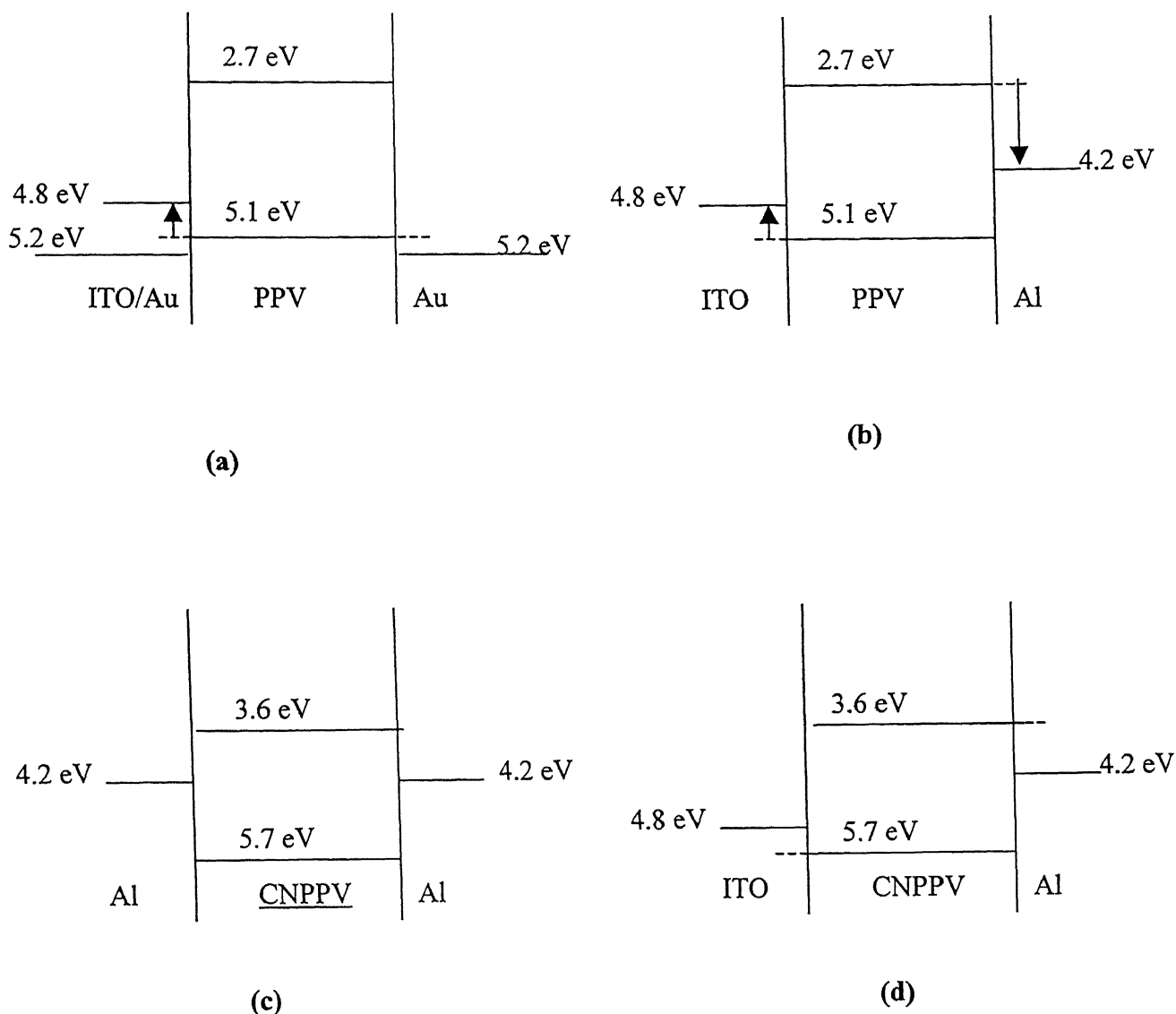Fig. 4.1: (a) Band diagram of hole only PPV base devices. In these both electrodes (ITO or Au) has a work function (4.8 or 5.2 eV) [55] closer to HOMO level (5.1 eV) of PPV. (b) Band diagram of dual charge carriers, PPV based devices. Here work function of Al (4.2 eV) [55] lies closer to LUMO level of PPV. (c) and (d) Band diagram of electron only and dual charge carriers, CNPPV based devices. HOMO and LUMO levels of CNPPV lie at
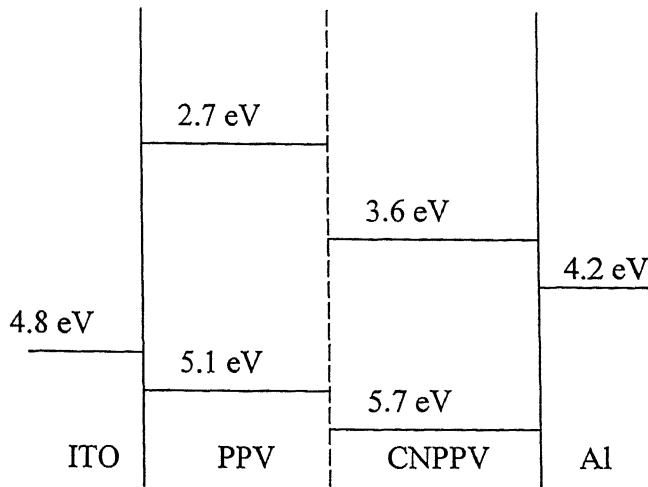
Fig. 4.2: Band diagram of PPV and CNPPV based multilayer device structure, which is used in determination of mobility from EL transient. [56]

[4.1] PL Characterization of PPV and CNPPV Material:

Thin films of these polymeric materials PPV and CNPPV were characterized using photoluminescence spectroscopy. PL spectra for PPV and CNPPV thin films are shown in Fig. 4.3 and 4.4 respectively. This spectrum is taken from ITO side of the device. For PPV thin films concentration of solution used was 18 mg/ml and for CNPPV it was 7 mg/ml. The excitation source used for PL measurements is He-Cd Laser with excitation wavelength 442nm and PL was recorded using a fiber optic spectrometer. We see that band gap of PPV lies in green region and that of CNPPV lies in red region of the visible spectrum. This makes these materials useful for green and red light emission. The PL spectra match well with standard spectra [57,58] of the materials complete with phonon replica and zero phonon transition at 511.5 nm and 603 nm for PPV and CNPPV, respectively. From features of PL spectrum of both materials we can conclude that the material, which we are using for fabrication of devices, is of high quality.

39

Fig. 4.3: Photoluminescence spectrum of PPV thin films used in fabricating PPV based devices. The characteristic peaks occur at 511.5 nm and 545 nm respectively.

Fig. 4.4: Photoluminescence spectrum of CNPPV thin films used in fabricating devices. Characteristic PL peal occurs at 603 nm.

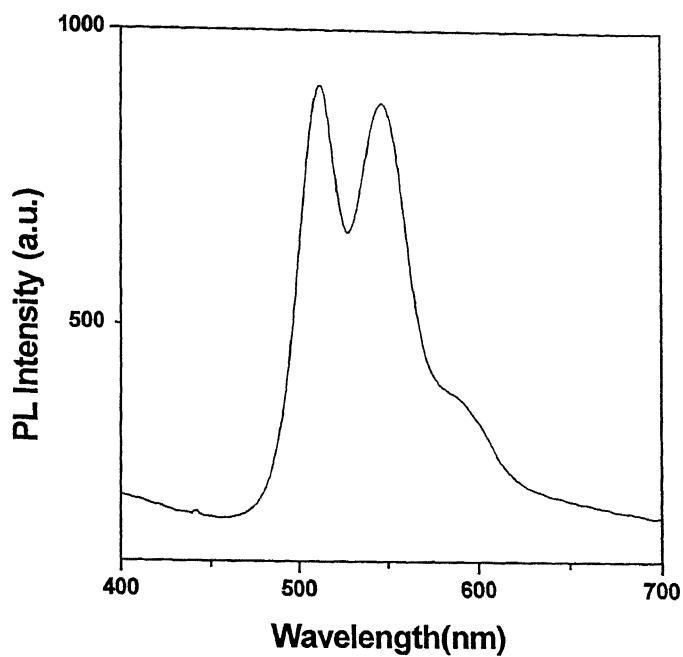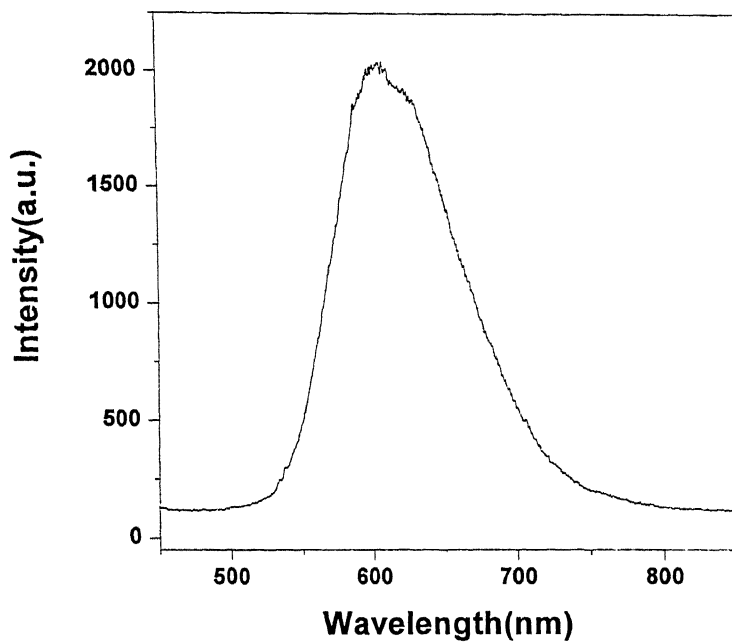## [4.2] Current-Voltage Characteristics:

[a] Hole only devices using PPV polymer layer:

In this section we concentrate only on forward bias characteristics since that is important from the point of view of mobility consideration. Further, reverse bias characteristics in these devices is known to have leakage problems leading to unwanted memory effects in electrical measurements. In order to study the transport of holes in PPV, two kinds of device structures, (1) ITO/PPV/Au 'sandwich', and (2) Au/PPv/Au 'planar' were used. In sandwich structure the polymer layer was coated twice and coating of Au cathodes was done by giving a flash rather than slow evaporation in order to get stable devices evaporated. Thickness of polymer film is approximately 150nm, whereas in planar structure a gap of 100 μm is kept between the two gold (Au) electrodes. Since the work function of Au and ITO matches with the HOMO level of PPV (as shown in Fig. 4.1(a)), we expect only holes to be injected from both electrodes. Thus the only carrier entity is hole that moves under the application of bias field. Injection of electrons is thus restricted by proper choice of anodes and cathodes.

Fig.4.5 shows the linear current-voltage characteristics (inset is double logarithmic plot) of the *sandwiched* ITO/PPV/Au device. Fig. 4.14 (described at the end of this section under planar device structures) shows both the linear and log- log plots of current – voltage characteristics for *planar* Au/PPV/Au device. From the slop of logI vs. logV plots, in both the cases, we can observe that current depends quadratically on voltage. This behavior is characteristic for space charge limited current (SCLC) in which case current density is usually related to voltage by following expression [18]

$$J = (9/8)\ \varepsilon_0\varepsilon_r\mu_p\ (V^2/L^3) \tag{4.1}$$

All the symbols are explained in chapter 2. The importance of the observation of space charge limited current in our hole only devices is that it shows that hole current is bulk limited and not injection limited. However any deviation observed from a factor of 2 can be explained by dependence of mobility of charge carriers on electric field and/or presence of traps due to imperfections, cross links, and kinks present in the polymeric material. Ohmic nature of current (i.e., J α V) is observed at very low bias, where injection of charge carriers is not taking place. Contribution to current may come due to presence of a few thermal charge carriers.
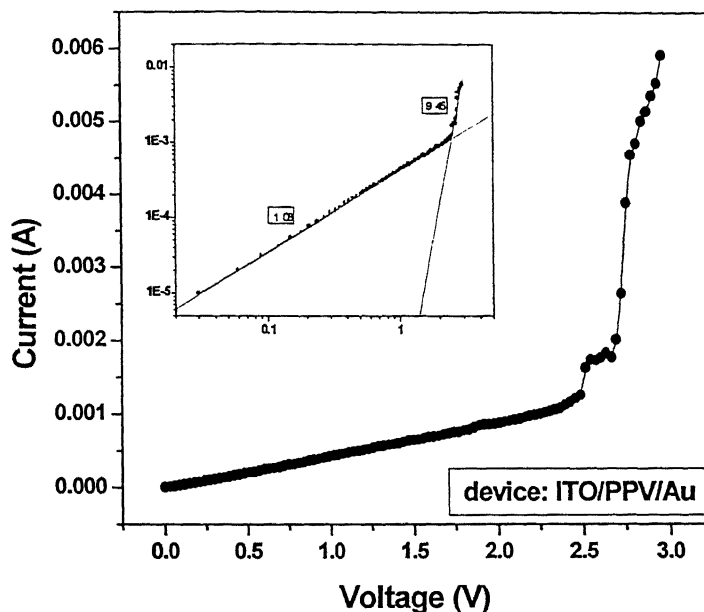
Fig.4.5: Typical current-voltage forward characteristic of ITO/PPV/Au device. Inset is the log-log plot of the same. It shows a turn on voltage of 2.75V and two regions with slopes 1.08 and 9.45

[b] Double charge carrier devices using PPV polymer layer:

In order to study charge transport in a real OLED, sandwiched structures of ITO/PPV/Al were fabricated. This is the typical class of structure which is suitable for PLED application. A precursor solution 18mg/ml was used to make approximately 100nm thick films of polymer. ITO injects holes in the polymer and since, work function of Al matches with the LUMO level of PPV, Al injects electrons in the polymer. Fig. 4.7 shows current –voltage characteristics (double liner and double logarithmic plots) of singly coated PPV devices. From slope of logI vs. logV plot it is clear that current depends quadratically upon the applied bias, which is again a characteristic of space charge limited currents (SCLC). We have observed similar dependence in hole only planar device. Since the current densities in these devices and hole only across devices, shown in Fig.4.5 are comparable, this suggests that in case of PPV the contribution to current due to electrons is negligible. Since electrons are severely trapped in PPV, the charge transport or current conduction is dominated by holes only. Similar current

42

– voltage characteristics were obtained from many device structures fabricated under similar conditions during the course of this work. However, turn on voltage varies from 0.8 to 1.5 V and the slope of second region in case of logI vs. logV plot varies from 1.7 to 3. However, many of the devices with a single coat of PPV turned out to be shorts. Due to this reason double coating of PPV was tried and devices with double coating of PPV were fairly stable. In this case the thickness of polymer layer after double coat is approximately 150nm.

Fig. 4.8 shows the current – voltage characteristics of a doubly coated PPV device. It is clear that the turn on voltage is around 6V as compared to single coat device in which it is 1.25 V. Also the current density values for the same voltage are much smaller double coat device as compared to single coat. This is due to increased resistance with increase in film thickness.

For a double charge carrier device one has to take into account both space-charge (holes) and trapping (electrons). Hence, for such a device two additional phenomena become important, which are namely, (1) recombination, and (2) charge neutralization. Due to charge neutralization the total charge may far exceed the net charge. Due to this, the current density in a double carrier device may be larger than those in a single carrier device. This difference can be seen from comparison of current densities in hole only (Fig. 4.4) and double charge carrier (Fig. 4.8) device. In a simple case of no traps and field independent mobility the current density in case of double charge carrier device can be given by[17]

$$J = \left(\frac{9\pi}{8} \right)^{1/2} \varepsilon_0 \varepsilon_r \left(\frac{2q\mu_p\mu_n(\mu_p + \mu_n)}{\varepsilon_0\varepsilon_r B} \right)^{1/2} \frac{V^2}{L^3} \qquad (4.2)$$

where, factor B is the bimolecular recombination constant. ε_0 is permittivity of free space and ε_r is materials dielectric constant. μ_p and μ_n are mobilities of holes and electrons. L is thickness of the polymer layer sandwiched between two electrodes
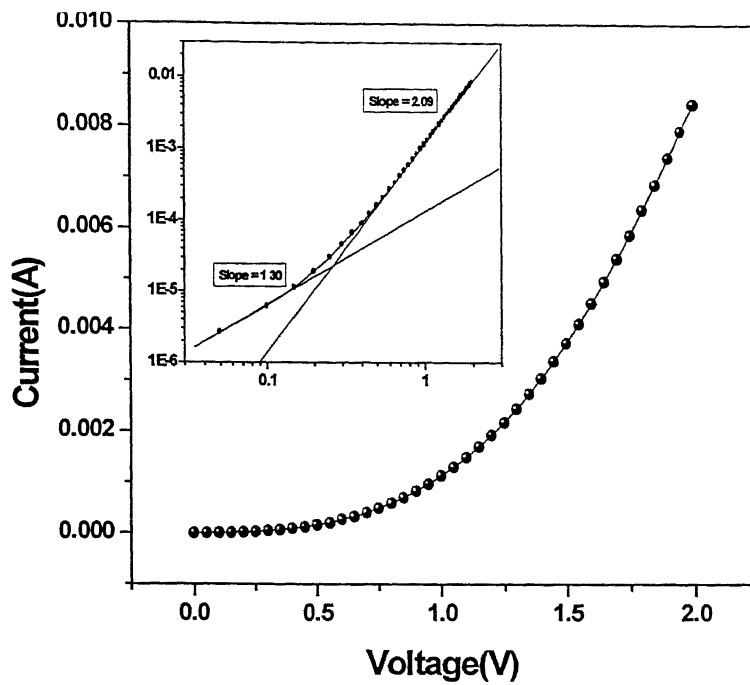
Fig. 4.7 : I-V characteristic of an ITO/PPV/Al device with single coating of PPV. Inset is the log-log plot of the same. In this device turn on voltage is 0.85 V and slope of two regions in log-log plot are 1.3 and 2.1 respectively.

Fig.4.8: I-V characteristic of ITO/PPV/Al device with double coat of PPV, approximate thickness of polymer film is 150nm. Turn on voltage of this device is 6V. Inset is log-log plot of the same. However here slope of second region is exceptionally high, it is 39.5. A clear dependence of current densities and turn on voltage on thickness (single and double coat)of polymer film can be seen from comparison with Fig.4.7.

44

Thus, in case of PPV charge transport is dominated by holes and current is space charge limited. Current densities are slightly higher in case of a double charge carrier device as compared to a single charge carrier device, mainly due to charge neutralization. From these I-V plots as shown above, we can see that there are regions of different slopes in double logarithmic plots. First region, J α V with slope approximately 1 is common to all of them. However, the slope of second region varies from 2 to 3 in case of single coat of PPV and very high slopes varying from 9 to 40 are observed in case of double coat of PPV layer. In some of the double coat devices we have also seen a region of slope 3 before the higher slope region (see Fig. 4.9). But in case of single coat structures the slopes have always been less than 3. Regions with slope 2-3 are SCL regions with a field dependent mobility, whereas appearance of very high slope regions in case of double-coated devices may be attributed to presence of traps and the abrupt increase in current can be attributed to trap filled limit. However, it is not clear as to why double-coated devices would introduce significantly more traps than single coat device. This may be related to variation in drying schedule for thick films.
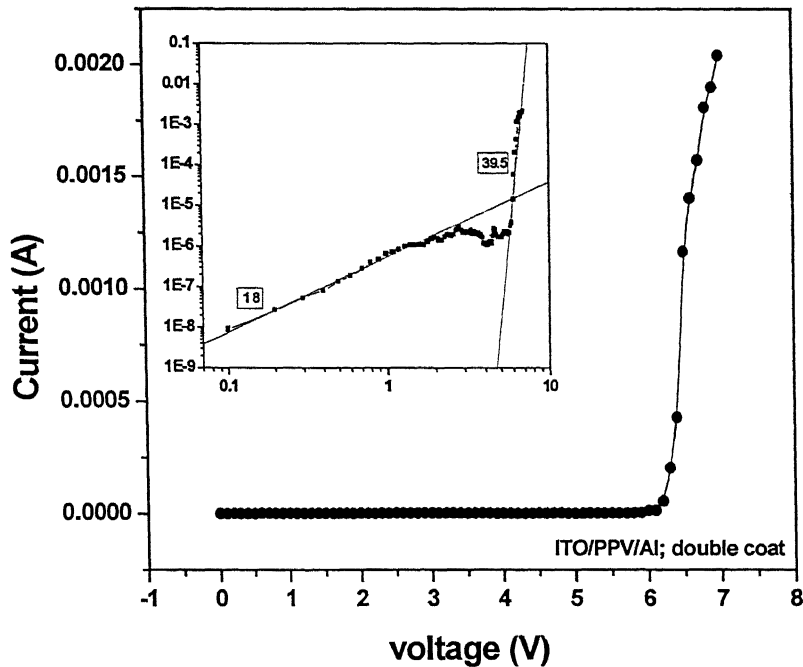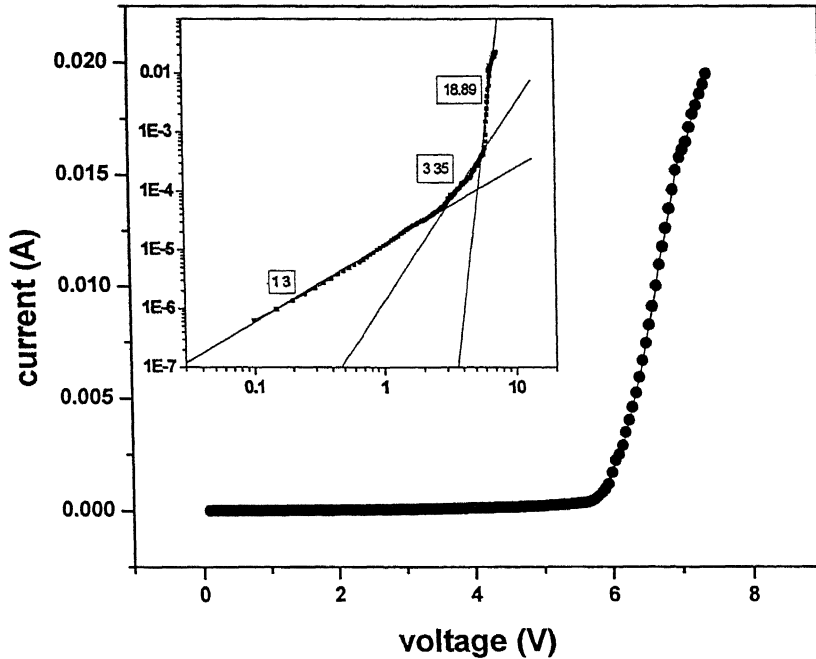

Fig.4.9: I-V characteristic of another ITO/PPV/Al device with double coat of PPV, expected thickness of polymer film is 150nm. Turn on voltage of this device is 6V. Inset is log-log plot of the same. However, here three regions appear in log-log plot, one having slope 1.3 other having slope 3.3 and third one again shows very high slope 18.89, like the previous one.

[c] Electron only device using CNPPV polymer layer:

From literature it is well known that unlike PPV, CNPPV facilitates the motion of electrons and hence it is used as an electron transporting layer in a multilayer PLED. In order to study the transport of electrons in CNPPV, electron only device with sandwich structure Al/CNPPV/Al, were fabricated. Current – voltage characteristic of Al/CNPPV/Al device is given in fig. 4.10. The initial slope I 1.6 rising to 6.8 in injection regime. Initial part of the curve does show evidence of field dependent transport but weaker than in case of trap free transport. Clearly, the transport of electron in CNPPV is dominated by the presence of traps.
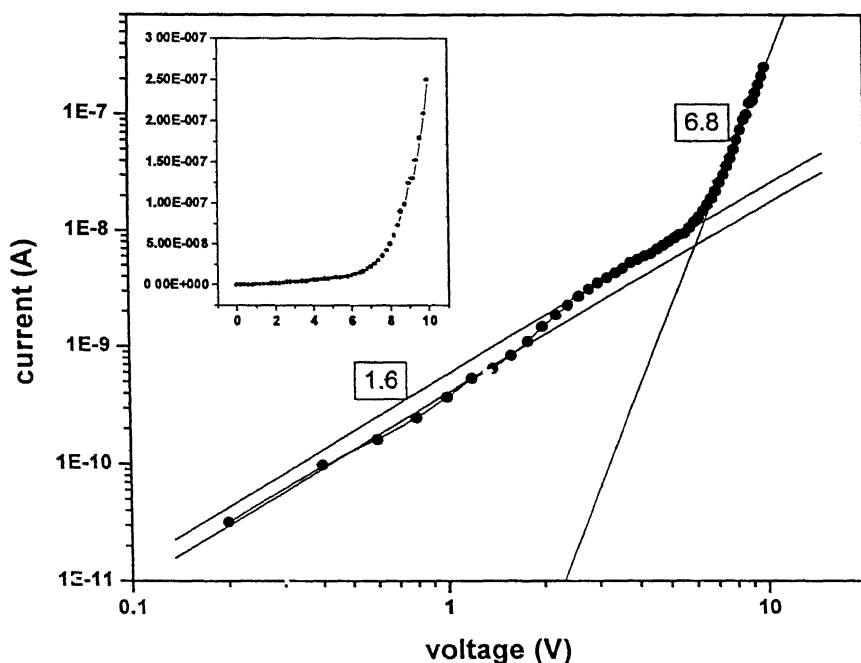

Fig.4.10: I-V characteristics of CNPPV thin film used in electron only device. Turn on voltage is 7 V and in log- log plot there are two prominent regions with slopes 1.6 and 6.8. Inset shows the linear I-V plot of the same. These CNPPV thin films were deposited from a higher concentration (1o mg/ml) solution.

[d] Double charge carrier device using CNPPV polymer layer:

Current – voltage characteristics of a double charge carrier device (ITO/CNPPV/Al) is given in Fig. 4.11. It shows a very good rectifying behavior with a turn on voltage of 6V. From the inset log-log plot we can see three different regions with slopes 1, 2.2 and 7.1. However, the SCL region with slope appears for a very short range of voltage. The high slope region is due to current rises beyond trap filled limit. Similar characteristic is also observed in doubl-coated PPV based devices. In case of trap filled limit current density is given by following expression [16]

$$J = N_c e\mu \ (\varepsilon_0\varepsilon_r/qN_t)^r \ (V^{r+1}/ \ L^{2r+1})C(r) \qquad (4.3)$$

with r, being trap distribution parameter. Above expression is very well described in chapter-2 of this work. Basic feature of I-V characteristics of CNPPV based devices is that current is trap limited.
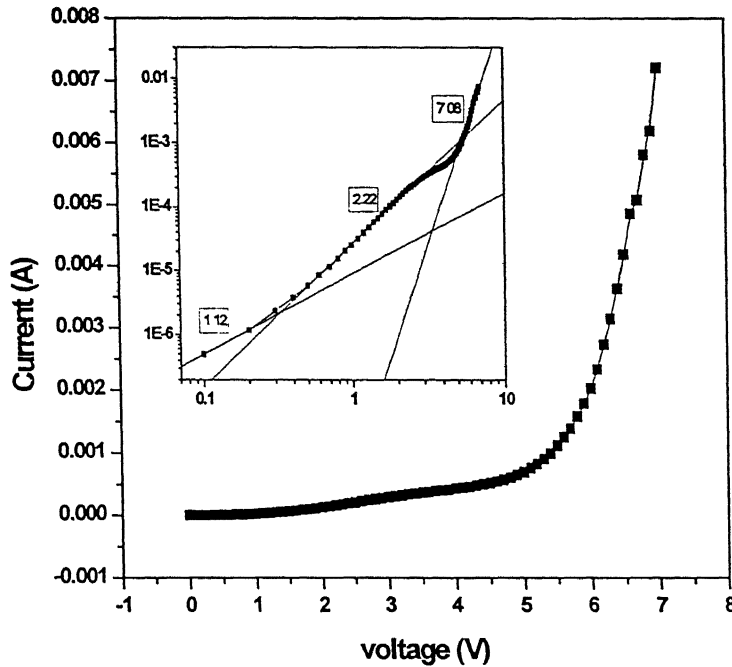

Fig.4.11: I-V plot for an ITO/CNPPV/Al device. Inset shows log-log plot of the same. It shows a turn on voltage of 6V. And there are three distinct regions in log-log plot with slopes 1.12, 2.2, and 7.08.

47

[e] I – V Characteristics of Planar Structures:

In this section we show measured I – V curves in two types of planar structures for hole only devices in PPV. Fig. 4.12 shows such curves for three different devices with two different spacings for evaporated Au electrode on the top of PPV film. For 100 μ devices the current remains contact limited with blocking contacts. For a separation of 60 μ, however, we see switch over from blocking resistance to bulk resistance. No injection regime is seen in this range of voltage.

Fig.4.12: This is I-V plot in case of Au/PPV/Au planar device structure. Au is the top electrode. There are two electrode separations 60 micron and 100 micron. I-V in case of two different 100-micron separation devices is plotted in graph. Initial slope in each case is ~10^8 whereas, next slope, that appears only in case of 60 micron electrode separation is 0.5×10^9. Here we have not gone to injection regime of conduction.

I – V characteristics for similar planar devices with ITO contacts at the bottom separated by different spacings is shown in Fig. 4.13. Near ohmic behaviour is observed in these samples upto 110 V. Hence these structure require much larger voltages to obtain injected charge carrier transit time.

However, these device structures show space charge limited current beyond 800 V for a 100 μ separation (i.e., field required to cause injection should be higher than 8 x 10⁴ V/cm.). Fig. 4.14 shows such a I-V characteristic for a 100 μ, with gold electrodes on top of PPV layer. It shows injection regime after 800 V has been crossed. Appearance of slope 2.2 after injection shows that current becomes space charge limited in the injection regime. Hence to be able to use these for transit time studies using voltage pulsing one needs a high voltage pulse generator.

Fig.4.13: This is I-V plot for a planar ITO/PPV/ITO device structure. ITO is bottom electrode unlike Au on the top. There are three different electrode separations, 100, 150 and 200 micron. Here also devices have not gone to injection regime of charge carrier transport.
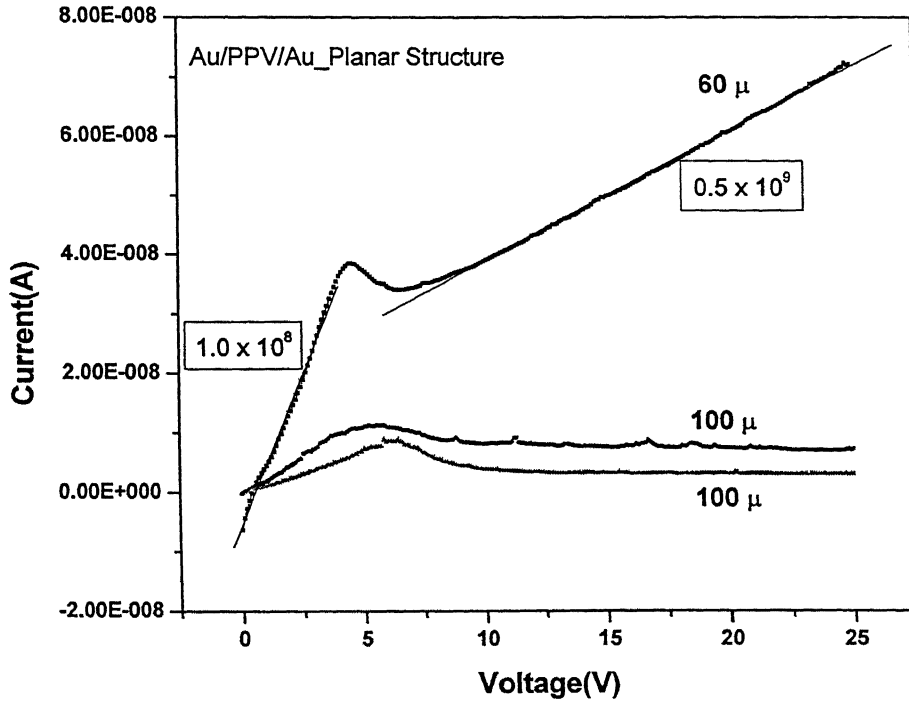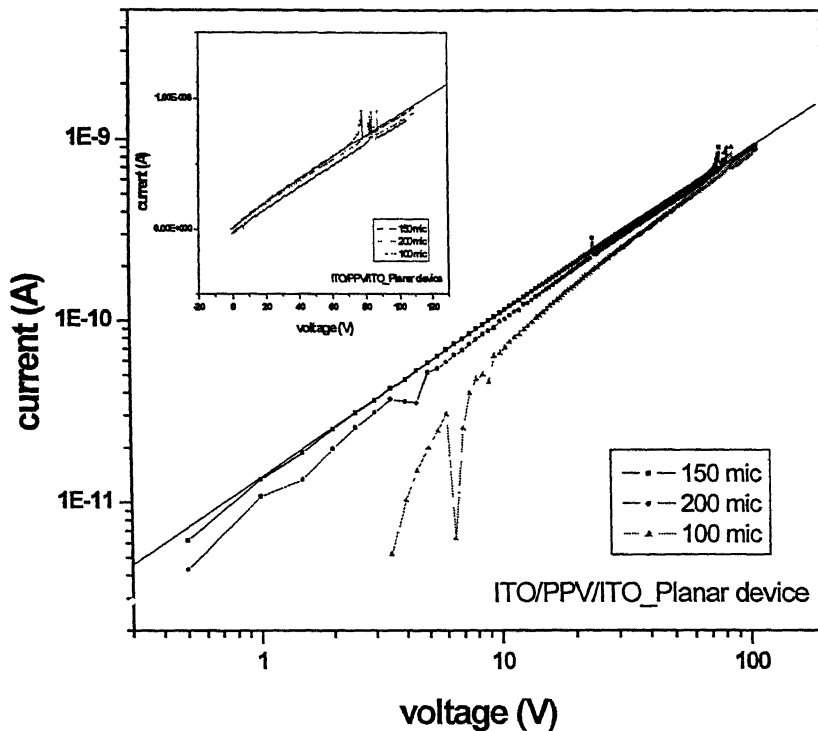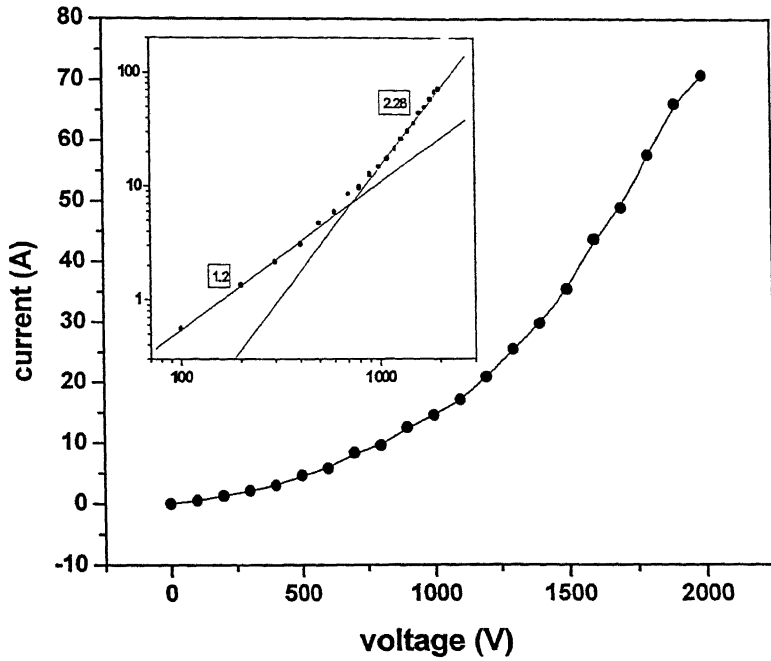
Fig.4.14: This is I-V plot in case of Au/PPV/Au planar device structure. Au is the top electrode. Electrode separation is 100 micron. In this case I-V is taken upto 2kV in order to achieve injection regime. From inset log-log plot it is clear that injection starts after 800V. There are two different slope regimes with slopes 1.3 and 2.25.

Salient Features Common to I-V Characteristics:

Some of our key observations from forward I-V characteristics are listed below

- In all the I-V characteristics we have observed an initial region with slope 1 – an apparent ohmic region. It may be present due to presence of thermal charge carriers. However, it is known that in case of many insulators, even in absence of requisite thermal carriers one obtains empirical $J \propto V / L^3$. This region is often confused with pure ohmic current with thermal carriers.

- In case of single-coat PPV devices we have observed injection region with slope 2 to 3 in log – log plot. Slope 2 signifies that current is space charge limited. Variation of slope from 2 to 3 can be understood by means of field dependence of charge carrier mobility. This is the region of interest for extracting mobility and its field dependence.

50

- In case of double-coated PPV devices, we have observed very high slopes, which can be attributed to presence of traps in case of these devices, though the origin of traps is not clear.
- In case of CNPPV devices, current rise due to trap filled limit is clearly observed.

To determine mobility from I-V characteristics, we have considered only that region of I-V that shows effect of mobility. All the I-V showing higher slopes (indicating dominance of traps) have not been used for this purpose.

[4.2] Mobility of charge carriers from forward current – voltage characteristics:

[a] Hole mobility in PPV based PLEDs:

Since from current-voltage characteristics of single and double charge carrier devices it is clear that in PPV charge transport is dominated by holes with negligible contribution to current from electrons. With this observation we can easily assume that it is the movement of hole that dominates the I-V characteristics. Thus, we can use I – V characteristics of either single charge carrier device (ITO/PPV/Au) or double charge carrier device (ITO/PPV/Au) to determine the mobility of holes by fitting I- V plot to equation (4.1). However, the slope of logI vs. log V plot in SCL regime differs from quadratic behavior and which can be attributed either to field dependence of mobility or due to presence traps in material. In such a case fitting of I vs. V plot from equation (4.1) may not give correct values of mobility. Recently a differential method has been proposed by Natali *et. al.* [40] to determine the mobility of charge carriers from I-V characteristics. The method boils down to computation of mobility from

$$\mu(\mathcal{E}_c) = \frac{L^3}{\epsilon} \frac{J}{V^2} \left(\frac{p^2}{p+1} \frac{1}{1 + \frac{1}{p} - \frac{1}{p} \frac{d\ln p}{d\ln V}} \right) \tag{4.3}$$

where L is the thickness of polymer layer sandwiched between two electrodes, ε is permittivity of the polymer material, and p denotes the slope of log J vs. log V plot.

The assumptions made in getting the above expression are:

- There is one charge carrier entity present in the material or device.
- Material is free of traps.
- Current conduction is limited by space charge.

For a valid application of this method, it is important to ensure these conditions. However, the advantage of this method is that specific dependence of current on voltage need not be known. The basic assumption that we are using is that material is free from traps. In order to satisfy the assumptions made by Natali, mobility is calculated at first from a hole only device in PPV. The device structure used for calculation of mobility is ITO/PPV/Au. Using this method hole mobility is calculated as a function of voltage. Further it is extended to calculatin of hole mobility in double charge carrier devices on the basis of assumption that current conduction is hole dominated in PPV films. Fig. 4.15 shows mobility as a function of electric field for a hole only ITO/PPV/Au device structure. Hole mobility in PPV devices come out to be 10^{-5} to 10^{-4} cm^2 / V.sec, which is comparable to values given in literature for PPV material from different experimental techniques. This graph plots Log μ as a function of $\sqrt{E}$, which is a straight line. This kind of field dependence is known popularly as Poole Frenkel field dependence [59,60,61], which is a common feature observed in PPV and other polymeric materials used for PLED application. This field dependence can be expressed by means of following expression

$$\mu = \mu_0 \exp \left(\sqrt{\frac{E}{E_0}} \right) \tag{4.4}$$

where μ_0 is zero field mobility.

Fig. 4.16 (a) and (b) show J-V characteristics and mobility calculated from J-V characteristics respectively. This is for a double charge carrier ITO/PPV/Al device. However, we see that mobility values are comparable to those obtained in a hole only device in PPV. Also the field dependence of mobility remains the same. From this we can conclude that our assumption that in PPV current conduction is dominated by holes is fairly correct. Hole mobility in these devices also exhibits P-F kind of field dependence with zero field mobility $\mu_0 = 3.4 \times 10^{-7}$ cm^2/Vsec $E_0 = 1.23 \times 10^4$ V/cm.
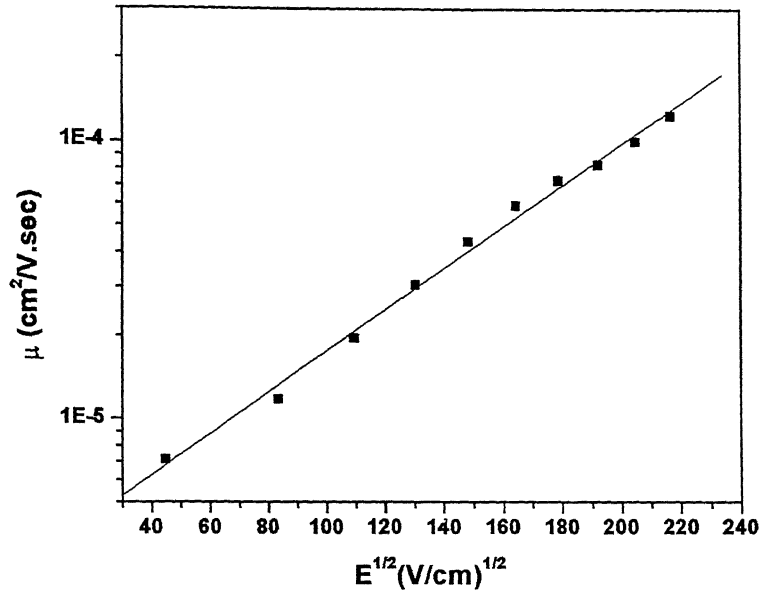
Fig. 4.15: Log μ vs. E $^{1/2}$ plot. Mobility is calculated from I-V data in SCL regime from hole only devices in PPV . Graph shows Poole Frenkel kind of field dependence with parameters $\mu_0 = 5.6 \times 10^{-7}$ cm^2/Vsec and $E_0 = 2.0 \times 10^4$ V/cm.

Fig. 4.16 (a) J vs. V plot of ITO/PPV/Al device. (b) Mobility calculated from SCL regime J-V data, as a function of electric field. We see a similar kind of field dependence as observed in case of hole only devices using PPV film with comparable values of parameters $\mu_0 = 3.4 \times 10^{-7}$ cm^2/Vsec and $E_0 = 1.23 \times 10^4$ V/cm.

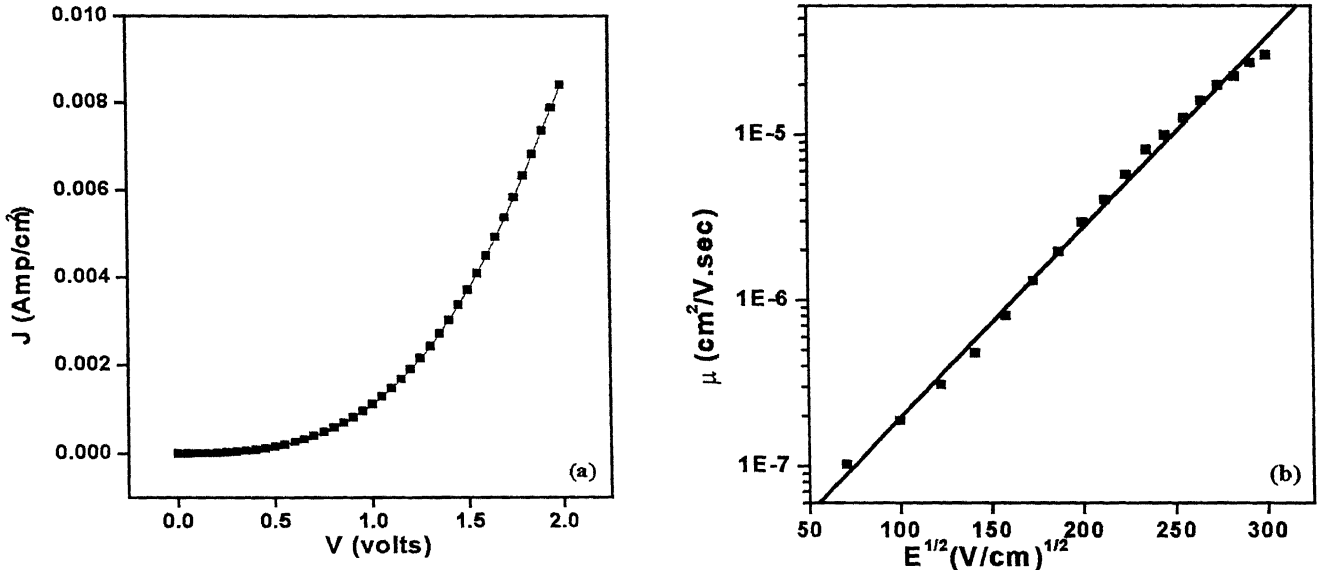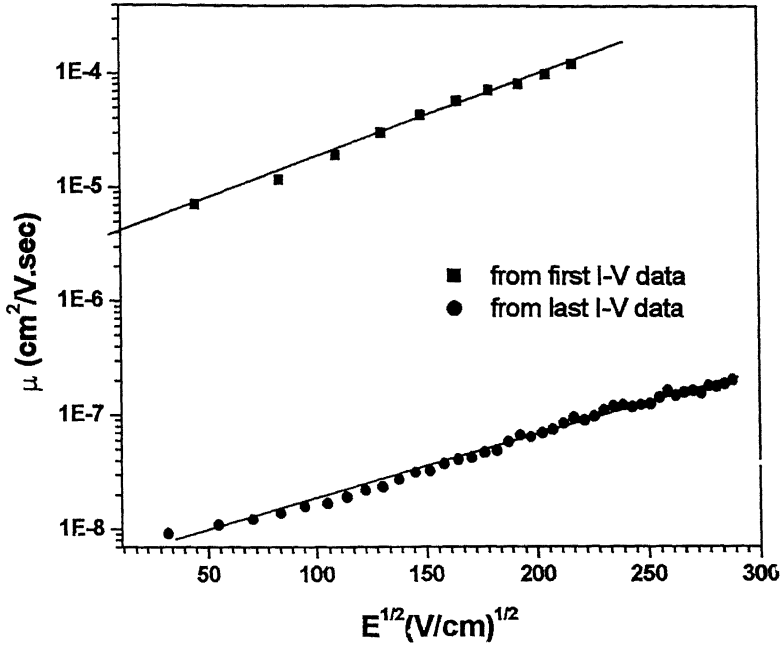Fig. 4.17: Mobility as a function of electric field in a hole only ITO/PPV/Au device. Two graphs shows mobility from the first I-V data and I-V data obtained at last after aging. With parameters $\mu_0 \approx 10^{-7}$ and 10^{-9} cm^2 /V.sec and E$_0 \approx 2.0$ x 10^4 and 3.1x10^4 V/cm respectively in fresh and aged I-V.

In Fig.4 17 we have shown mobilities as a function of electric field for the same device when it was fresh and from an I-V of the device had aged. In mobility calculated after aging , Poole Frenkel dependence is still observed with parameters $\mu_0 \approx 10^{-9}$ cm^2 /V.sec E$_0 \approx 3.1$x10^4 V/cm. We see that E$_0$ does not change whereas μ_0 changes significantly. The lesser values of mobility at similar fields are obtained in an electrically aged device. This reduction in mobility values can be caused as a result of degradation of material or that of contacts of material with electrodes due to aging. However, it is also possible that the observed reduced mobility is an effective one due to failure of accounting for degradation in contacts. The parameters of field dependence of mobility μ_0 and E$_0$ obtained are comparable those obtained in the literature in case of PPV material. We have presented a comparison of these parameters with literature values in Table 4.1 in a later section.

[b] Charge carrier mobility in CNPPV based PLEDs:

The forward I-V curve for this device structure has already been given in Fig. 4.11 in section 4.2 [d]. The middle region of the I-V curve has a slope of 2.22. This is the only region where Natali's differential analysis can be applied. The results of this analysis are shown in Fig. 4.18, where μ_0 and E_0 are observed to be $\approx 10^{-7}$ cm^2 /V.Sec and $\approx 10^4$ V/cm respectively. Surprisingly the values are comparable to those obtained for holes in PPV and conflicts with the known character of CNPPV as an electron transport layer.

This only points to the possible dangers of extending I-V differential analysis method by ensuring that the I-V is dominated by bulk transport. Hence we believe that influence of traps controls characteristics even in this regime of I-V for the case of CNPPV and thus results obtained may not reflect true mobility of charge carriers.
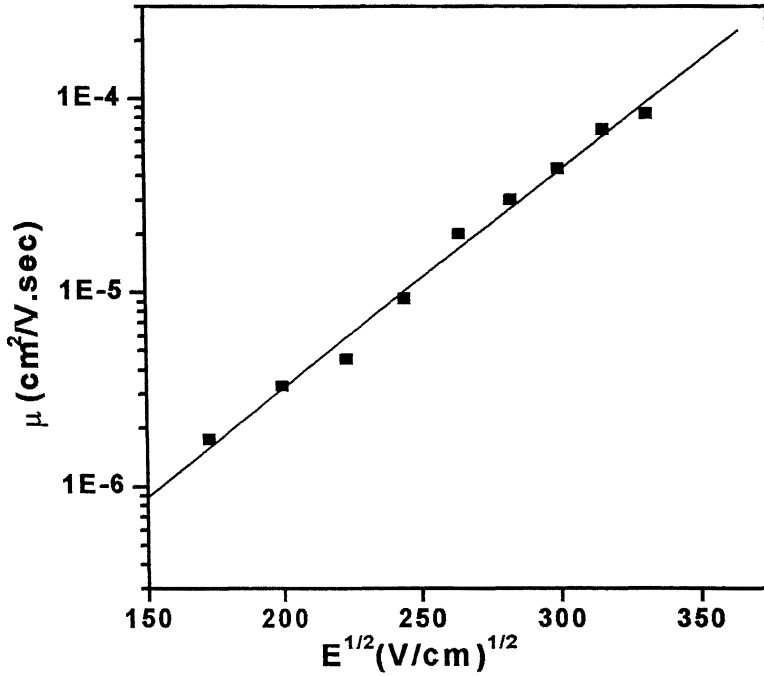

Fig. 4.18 Mobility calculated from J-V characteristics as a function of electric field for CNPPV material in ITO/CNPPV/Al device structure It also shows a PF kind of field dependence with parameters $\mu_0 \approx 10^{-7}$ cm^2 /V.sec $E_0 \approx 10^4$ V/cm.

Therefore, even in case of PPV, we need to use at least another method (of determining mobility) which does not depend on the assumption that the material is free of traps for its applicability.

[4.3] [a] Mobility of charge carriers from EL-transient:

When a voltage pulse of very short duration is applied to the device, the injected charge carriers take some time to reach recombination zone. This transit time can be observed in delayed electroluminescenece from the device. The delay time t_d observed in pulsed EL is related to mobility by means of equation

$$t_d = L^2 / \mu . (V-V_{bi})$$
(4.5)

where, L is thickness of polymer layer, V_{bi} is built in potential that comes out due to difference between workfunctions of two electrodes. Fig. 4.19 (a) gives EL response of ITO/PPV/CNPPV/Al device at three different voltage pulses of 1-μsec. duration. Note the shift in on set of luminescence with increase in bias. The delay time becomes lesser at higher voltages or higher electric fields. In Fig. (4.12) (b) delay time is plotted as a function of inverse of bias field. The bias field is corrected by a factor of V_{bi}, which is difference between work functions of two electrodes. The field due to built in potential, does not contribute to drifting of charge carriers so it is to be corrected in order to get correct mobility values. From the linear fit of t_d vs. $1/(V-V_{bi})$ plot, mobility comes out to 9.0×10^{-5} cm^2/V.sec. Fig. 4.20 (a) and (b) gives the EL transients and delay time in another similar device, which was unintentionally aged before taking the measurements. The mobility value observed in this device is 5.0×10^{-5} cm^2/ V.Sec. Decreased mobility in aged device may be again due to degradation of device due to aging, which is similar to the observed mobility values from current density vs. voltage in case of fresh and aged devices. Again comparable mobility values in case of ITO/PPV/Al and ITO/CNPPV/PPV/Al device structures suggests that in both the cases mobility observed is of the similar charge entity i.e., of holes. Fig.4.21 gives the mobility obtained from EL transient method as a function of applied electric field. It again shows a Poole Frenkel kind of field dependence as obtained in case of mobility calculated from J-V characteristics with $\mu_0 \sim 7.942 \times 10^{-7}$ cm^2 /V.sec $E_0 \approx 9 \times 10^4$ V/cm . These hole mobilities are consistent with those reported in literature for PPV.

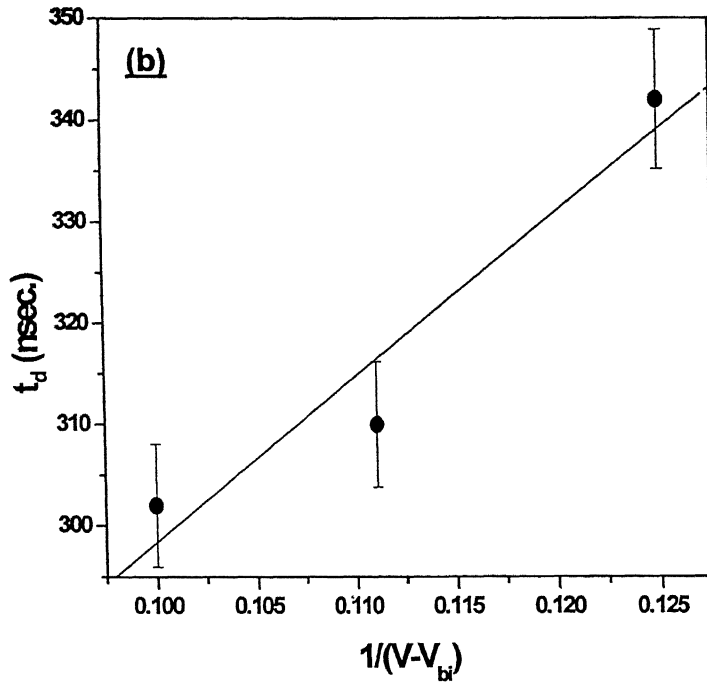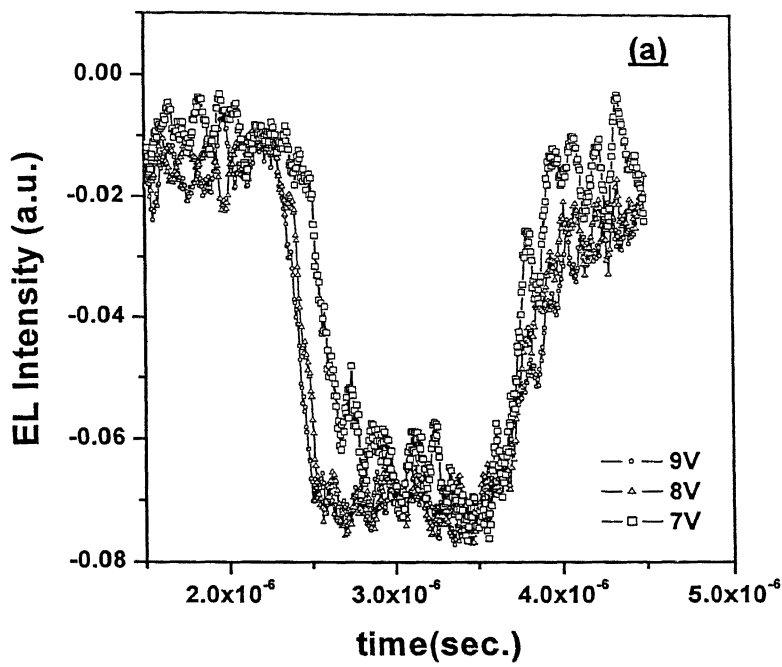Fig. 4.19: (a) Normalized EL intensity in a fresh ITO/PPV/CNPPV/Al device. EL responses at different voltage pulse heights are plotted in figure. The pulse duration is 1 μSec. (b) Plot of t_d vs. $1/(V - V_{bi})$. It shows clearly that as we increase the voltage pulse height, delay time decreases almost linearly.
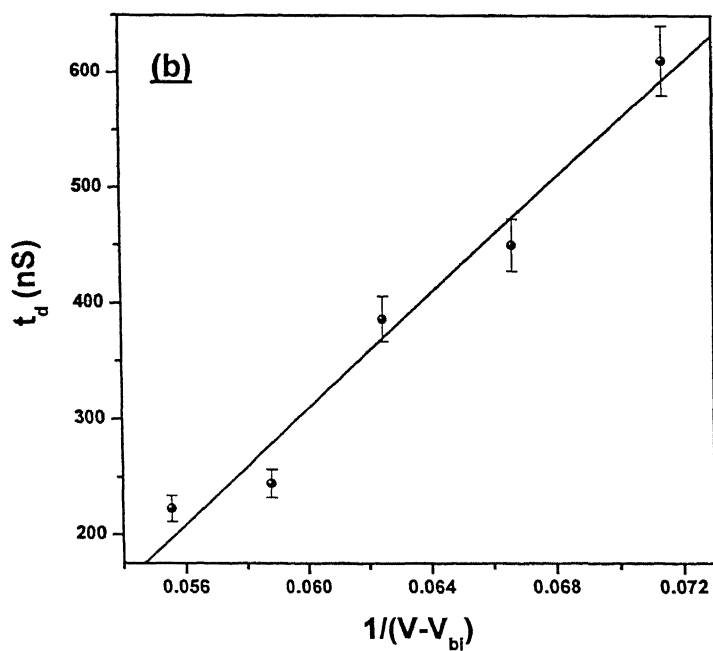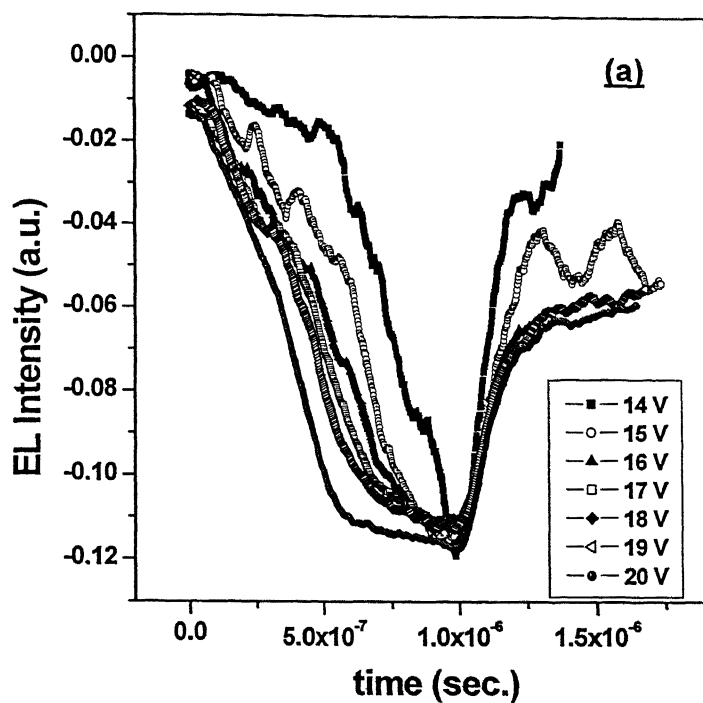
Fig. 4.20 (a) Normalized EL intensity in an aged ITO/PPV/CNPPV/Al device
(b) Plot of t_d vs. $1/(V - V_{bi})$
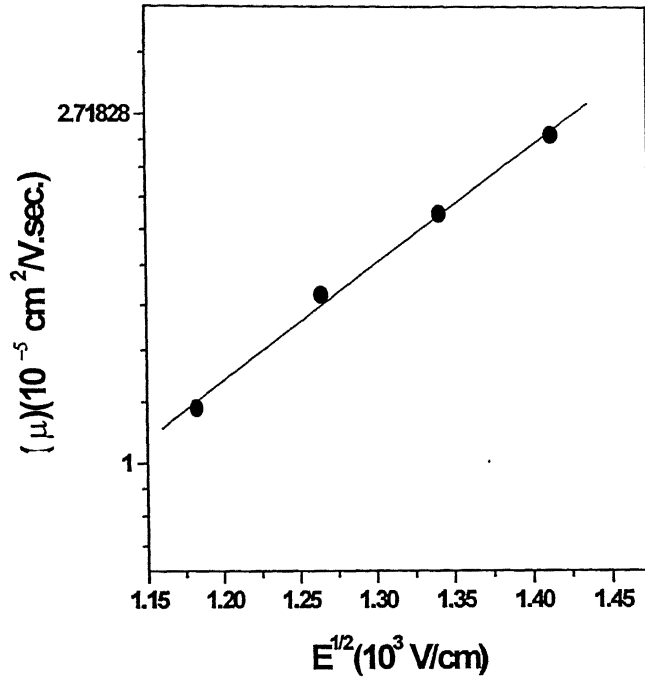
Fig. 4.21: ln μ vs. $E^{1/2}$, showing Poole Frenkel field dependence of mobility μ_0 $\approx 7.942 \times 10^{-7}$ cm^2 /V.sec $E_0 \approx 9 \times 10^4$ V/cm

The mobility measured in PPV in this work by the two methods is compared to those in the literature in Table 4.2. The mobility measured is comparable to to those reported from other groups, validates the quality of material and thin film processing steps being used in our group in the development of PLED structures. This has been one of the principal goals of this work.

[4.3] [b] Current Transients: An Important Precaution

In successfully doing the above experiment, it is extremely important that the current transient due to step change in voltage decays much faster than the duration of the observation of the experiment. In other words, the time constant of the circuit while measuring the EL transient must be lesser than the delay times observed. A typical current transient while performing the EL transient experiment is shown in Fig. 4.22 The current spike is due to C(dV/dt) and From linear fitting of Log of decay part of current, time constant comes out to be approximately 1(μSec)$^{-1}$, which is similar to

59

Reference	μ_0 (cm^2/V.Sec)	E_0 (V/cm)	Method
Blom *et.al.* [60]	~10^{-7}		J-V Characteristics
Martens *et.al.* [59]	$10^{-7} - 10^{-8}$	10^4	J-V Characteristics
Blom *et.al.* [24]	~10^{-6}		EL Transient
Ho *et.al.* [61]	6×10^{-6}		J-V Characteristics
Martens *et.al.* [43]	5.6×10^{-7}		Frequency Dependent Impedance
This Work	10^{-7}	10^4	J-V Characteristics
This Work	7.6×10^{-7}	8.9×10^4	EL Transient

Table 4.1: List of comparison of zero field mobility μ_0 and field dependence parameter E_0 in PPV thin films.

Reference	μ (cm^2/V.Sec)	Method
Lebdev *et.al.* [37]	~10^{-5}	Time of Flight
Blom *et.al.* [16]	0.5×10^{-6}	J-V Characteristics
Pichler *et.al.* [62]	~10^{-7}	Field Effect
Pinner et.al. [63]	~10^{-5}	EL transient
This Work	$10^{-6} - 10^{-5}$	J-V Characteristics
This Work	~10^{-5}	EL Transient

Table 4.2: List of comparison of mobility values in PPV thin films, collected from different sources.

RC value of circuit. So we can predict that current transients are even faster and in order to see devi current transient the RC factor has to be minimized. Also as we have seen in current decay there is i extra feature present, this may be described as dispersive transport of charge carriers So for tl device we can conclude that hole transport is dispersive in PPV polymer layer. In recent reports [b, for PPV and other polymeric materials, charge transport is found to be of both types 'dispersive' ai 'nondispersive' ,depending upon the processing of thin films of polymer.
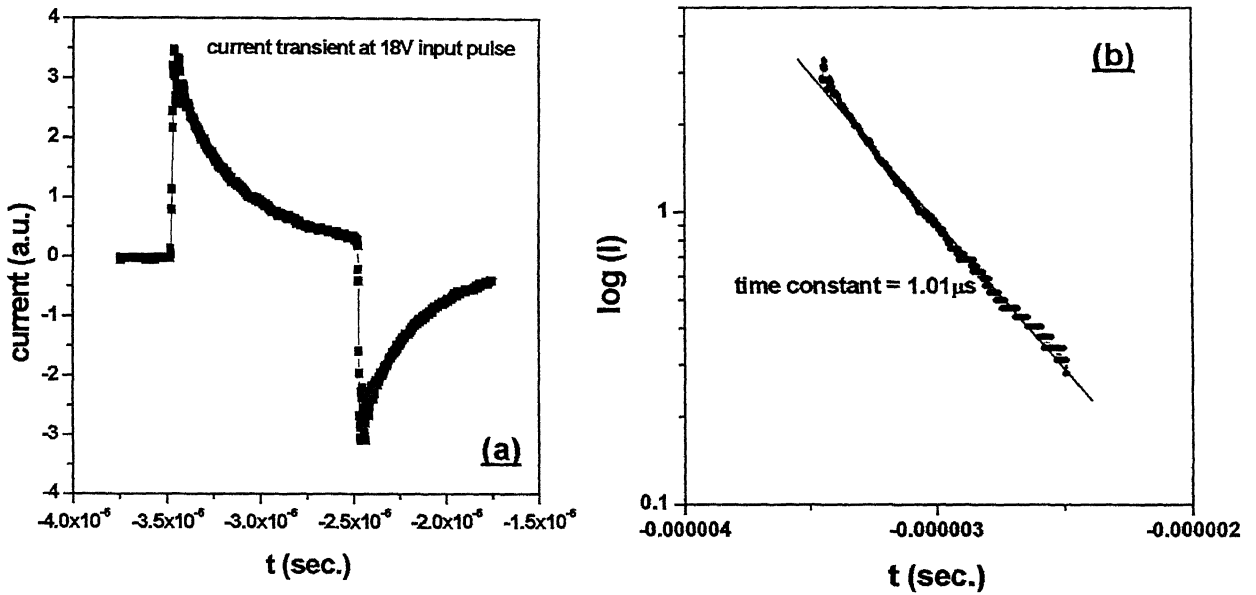
Fig. 4.22 (a) current transient at a voltage pulse of 18V in ITO/PPV/CNPPV/Al device
(b) Log I vs. t plot gives a decay time constant 1(μSec)$^{-1}$

[4.4] [a] Planar Structures: Current Transients

There has been at least one report for an electrode separation [39] of 200 μ in which the authors use current transient following voltage pulses across a planar structure. This has the advantage of simple experimental arrangement and direct interpretation. In our attempts to do similar measurements, we observe only current transients which do not display carrier transit characteristics

(a)

100mic

Current (A)

1E-9

110 V
100 V
90 V
80 V
70 V
60 V
50 V

time (sec)

150 mic_D_10Jan

Current (A)

1E-9

110 V
100 V
90 V
80 V
70 V
60 V
50 V

time (sec.)
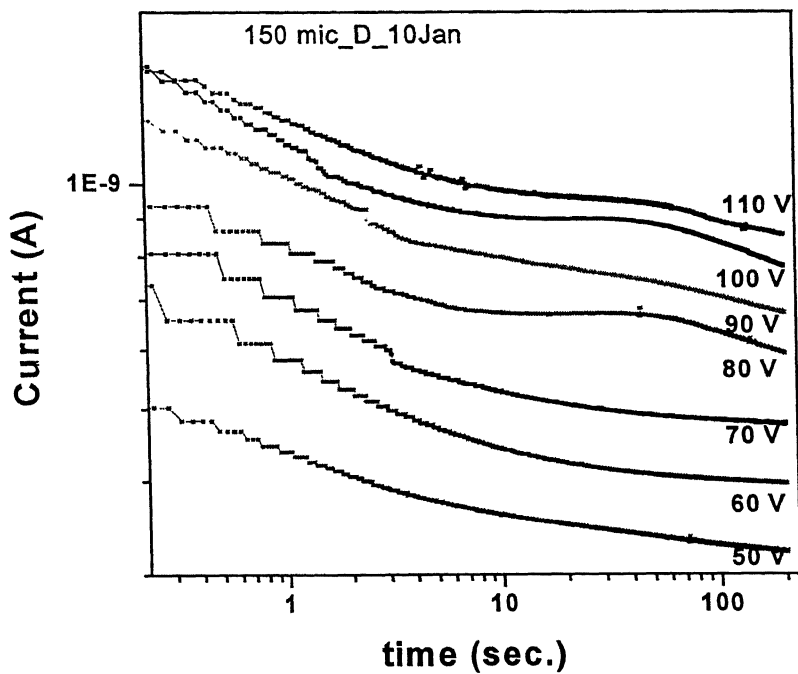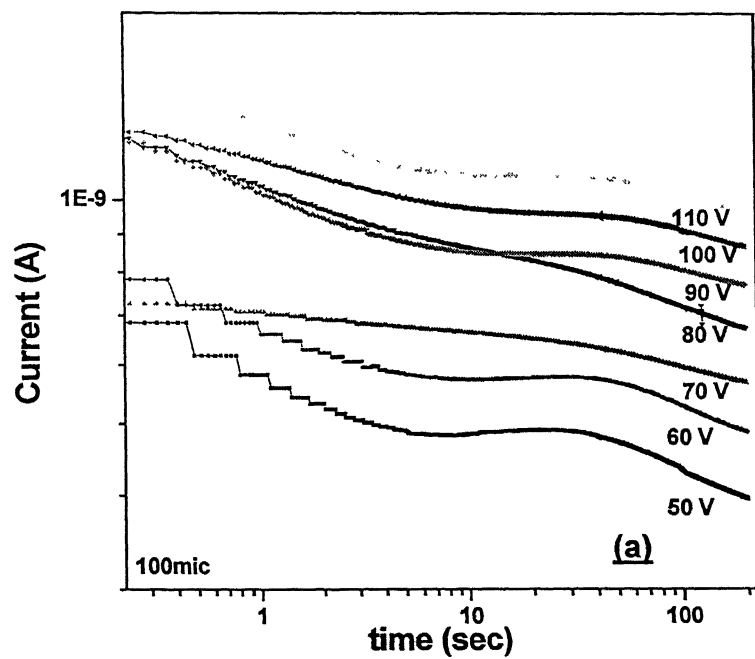
Fig. 4.24: Current transients as observed in case of planar ITO/PPV/ITO devices for three different electrode separations (a) 100 μ, (b) 150 μ and (c) 200 μ at different voltage step heights.

[4.4][b] Planar Structures: Open circuit Voltage Decay

In this series of experiments, the planar structures are first changed to a certain voltage, and then disconnected from the voltage source, short-circuit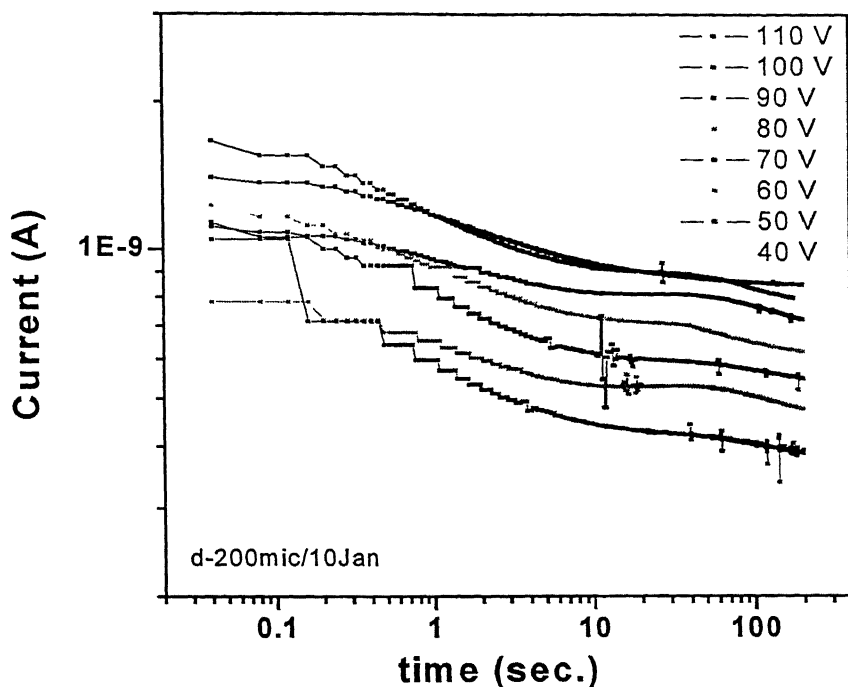ed for a fixed duration of time (1 hr.), and open circuit voltage monitored thereafter as a function of time. Fig. 4.25 gives open circuit voltage after charging of the Au/PPV/Au planar device. Here, open circuit voltage for five different voltage charging is presented. We observe a peak sitting over exponentially decaying open circuit voltages after 90V. In each case of voltage charging the decay profile of V_{oc} can be fitted to exponential decay with an appropriate choice of time constant. The decay of Voc is an indication of slow decay of stored changes in the device following charging. The store charges may be in the form of trapped charges or polarization either in the bulk or at the interface. Both the materials that we are dealing with in this study are non-polar, and hence interfacial polarizations and charging of deep traps are likely mechanisms of long lived charge storage.

64

Note that a surprising feature of the data is that the observed Voc is less for higher charging voltage. This indicates that the higher internal electric field (being more for higher charging fields) is able to drive out a larger fraction of the accumulated charges during the short circuit phase.
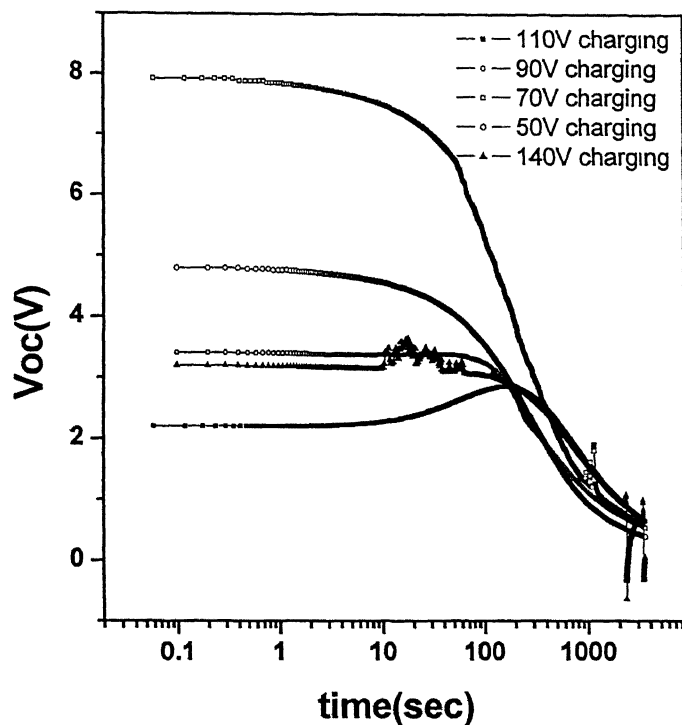
Fig. 4.25: Open circuit voltages at different charging voltages in case of Planar ITO/PPV/ITO device structure with 100 μ electrode separation.

It's the remaining charges, which contribute to Voc. Their decay is exponential with large time constants. However, also note that Voc peaks before finally decaying for higher charging voltage 90V and 110V. In Fig. 4.26 the decay over which the peak is superimposed is shown by fitting the baseline to an experimental decay. Fig. 4.27 shows the peaks extracted after baseline subtraction. The appearance of the peak is attributed to part of the accumulated charge redistributing itself under the action of internal electric field before decaying. The exact physical origin of the peak is unclear but must be found either in accumulation or polarization at the interfaces. The time constants involved and

Fig.4.26: Open circuit voltages after 100 V charging and fitting of baseline decay with time constant of decay being 1582 sec.$^{-1}$.

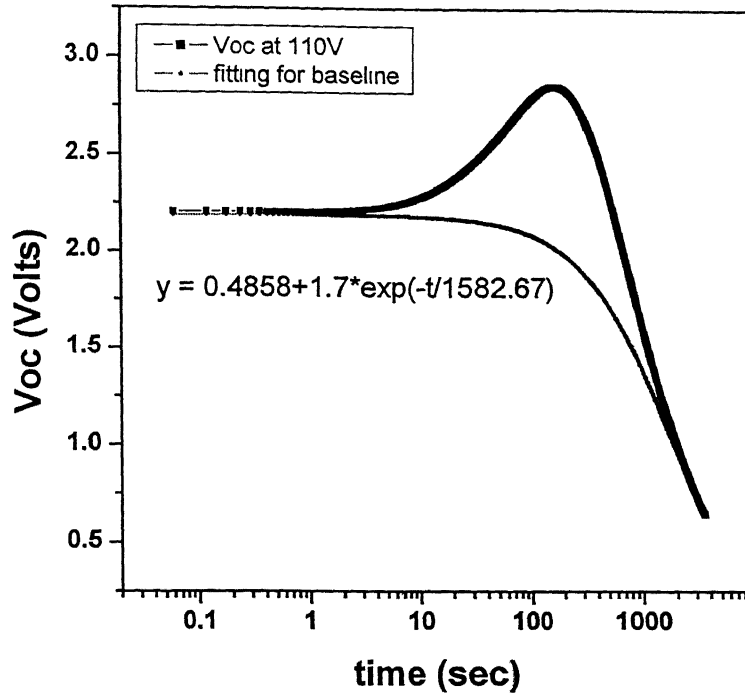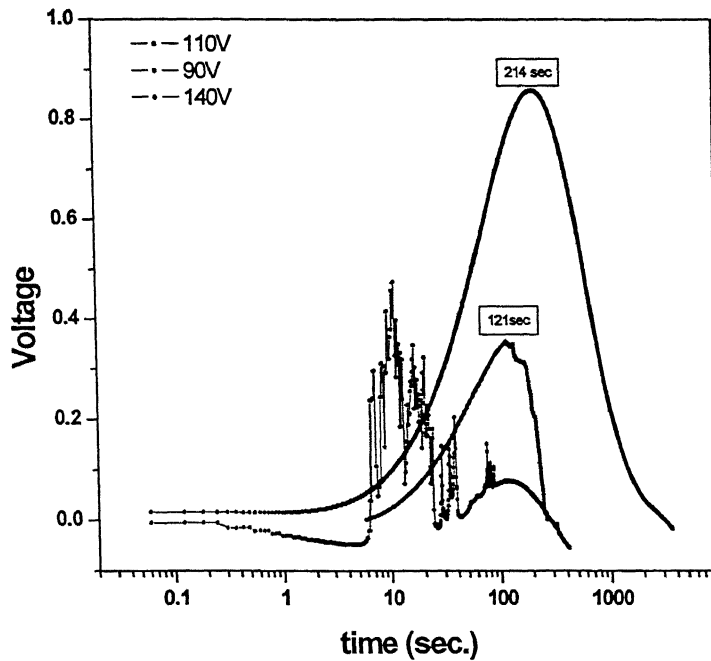Fig.4.27: Peak values in Voc, after subtracting baseline for three different voltage chargings. Here the decay time constants of Voc are 545 sec^{-1}, 1582 sec^{-1} and 1198 sec^{-1} respectively for 110V, 90V and 140V charging.

the peak times clearly indicate that long transit times of accumulated charges under the action of internal field is a common feature in these devices. This way of analysis provides an easy method of analyzing accumulated long lived charges in such devices. In a parallel work this method has been successfully used to study conventional PLED structure following degradation [manuscript by Vishal, Vineet and Y. N. Mohapatra is in progress].

[4.5] Development of internal electric field reducing effective barrier for injection and slow recovery with time:

Fig. 4.28 represents a series of forward I-V curves for two devices demonstrating observationof common phenomena in most of the devices during this study. After an I-V is recorded showing injection [shown as curve 1 in the Fig.], the next sweep shows as if there is no barrier and the current increases. However, the characteristics relax with time and tend to recover to the original curve to a large extent with a slightly increased threshold voltage.

We give a qualitative explanation to these consistently observed phcnomena in most of our devices. When the samples are kept under bias for long time or they undergo many dc bias sweeps, an internal electric field due to polarization is developed in the polymer layer. This internal electric field is directed such that it opposes the barrier for injection and soon device start showing no barrier for injection. As we have already, stated the origin of development of this internal electric field is either polarization or movement of ions within the polymer layer. Also it has been observed that this polarization or accumulation of ions slowly relaxes with time and the SCL nature of current-voltage characteristics is recovered with different turn-on voltage. The reversible part of polarization relaxes away with storage time. The increase in threshold voltage explained by charging of deep traps on forward biasing. However, this model needs further support from temperature dependent studies.

This phenomenon does impact conclusions about mobility from I-V measurements. It is the initial I-V curve that is the most suitable for "true" mobility measurements. Since one is not able to account for change in threshold voltage for injection properly for later curves, one obtains only an effective mobility. However, as shown earlier, it is the μ_0 which gets affected whereas E_0 remains the same for curves corresponding to degraded samples.
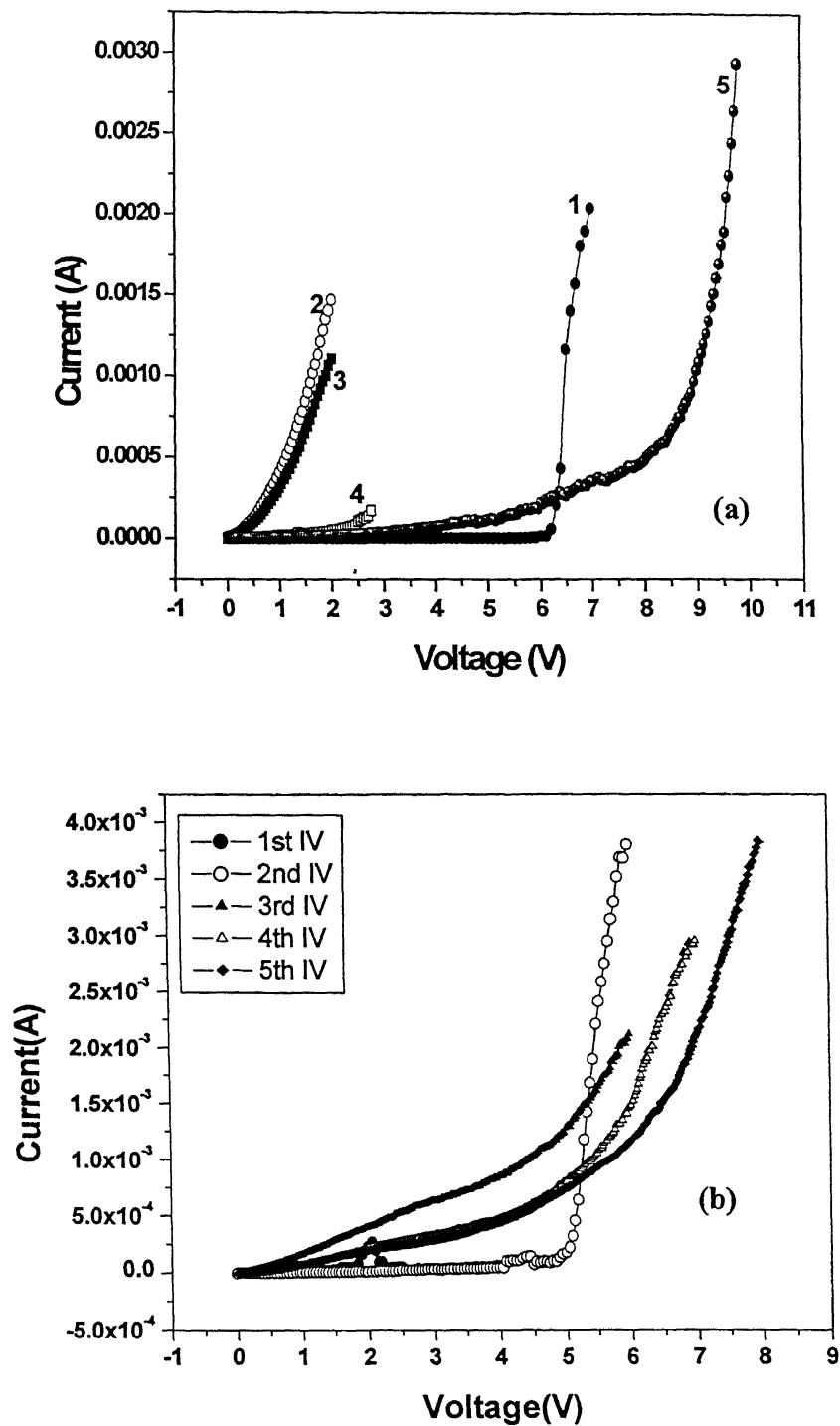
Fig.4.28: (a) Current-voltage characteristics of a double coated ITO/PPV/Al device and slow recovery, (b) similar kind of slow recovery as observed in a single layer ITO/PPV/Al device

68

The increasing importance of polymers in electronic and optoelectronic applications in the last decade has brought into focus methods of characterizing thin films of these polymer layers. Electrical characterization in terms of mobility and phenomena related to its measurement and determination has become central to efforts towards material development and device optimization. This work deals with such electrical characterization of two most important polymer materials PPV and CNPPV being developed for display applications at Samtel Center for Display Technologies, IIT Kanpur.

A variety of device structures including conventional sandwich structure for polymer light emitting diode applications were fabricated. Polymer Light Emitting Diodes using spin coating of PPV and CNPPV polymeric thin films with ITO acting as anode and vacuum deposited Al as cathode. In addition to these conventional sandwich structures, planar device structures were also fabricated for observing important phenomena related to charge carrier transport.

The most important objective of present work was to set-up experiments so as to be able to measure mobility in the polymer thin films as a validation tool for quality of material being used for PLED devices. This objective has been achieved for PPV thin films, and the mobilities measured by two different methods in our materials compare well with that of others.

Some of the main observations or conclusions of the work are listed below.

- In all the I-V characteristics we have observed initial ohmic region which may be present due to presence of thermal charge carriers. However, it is known that in case of many insulators, even in absence of requisite thermal carriers one obtains empirically for low fields $J \propto V / L^3$. This region is often confused with pure ohmic current with thermal carriers.

- In case of single-coat PPV devices we have observed injection region with slope 2 to 3 in log – log J-V plots. Slope of 2 signifies that current is space charge limited. Variation of slope from 2 to 3 can be understood by means of field dependence of charge carrier mobility.

- In case of double-coated PPV devices, we have observed very high slopes, which can be attributed to presence of traps in case of these devices. The origin of difference in behaviour for single and double coat devices remain unclear.

- In case of CNPPV devices, nature of current transport is dominated by presence of traps as indicated by the occurrence of trap filled limit in I-V curves.

- Mobility of holes in PPV is calculated from SCL regime of current – voltage characteristics of single layer PPV device, using (i) differential method, and (ii) from electroluminescence – transients obtained from multilayer PPV and CNPPV devices. Hole mobility obtained in this work matches well with mobility calculated by other groups. Mobility values obtained from these two methods are comparable and show Poole – Frenkel kind of field dependence. Typical mobilities measured for PPV is of the order of 10^{-5} cm^2/V.sec with $\mu_0 \sim 10^{-7}$ cm^2/V.sec and $E_0 \sim 10^4$ V/cm.

- Current density as well as apparent mobility goes down with degradation of the device. It is unclear at this stage whether this reflects degradation of material or change in field distribution in the device due to modification of interfacial charges.

- There is a clear signature of development of a persistent internal electric field in the device when it is subjected to successive dc biasing sweeps. This internal electric field reduces the barrier for injection and modifies I-V characteristics over long time scales.

- The appearance of internal electric field may be attributed either to polarization, charging of deep traps or to ionic space charge movement inside the polymer layer. However, I-V characteristics tend to recover towards original characteristics upon storage indicating spontaneous depolarization, slow emission from deep traps or drift of ions under the action of reverse internal field.

References:

1. M. Pope, H. Kallman, and P. Magnante, J. Chem. Phys. **38**, 2042 (1963).

2. W. Helfrich, and W. G. Schneider, Phys. Rev. Lett. 140, 229(1965).

3. C. W. Tang and S. A. Vanslyke, Appl. Phys. Lett. 51, 913(1987).

4. C. W. Tang, S. A. Vanslyke and C. H. Chan, J. Appl. Phys. 65, 3610 (1989).

5. G. Horowitz, D. Fichou, X. Z. Peng, Z. Xu, and F. Garnier, Solid State Commun., 72, 381 (1989).

6. F. Garnier, G. Horowitz, X. Z. Peng, and D. Fichou; Adv. Mater. 2, 592 (1990).

7. D. Braun and A. J. Heeger; Appl. Phys. Lett. 58, 1982 (1991).

8. P. W. M. Blom and M. C. J. M. Vissenjerg; Mater. Sci. Engg. 27, 53 (2000).

9. P. W. M. Blom and M. J. M. Dejong, C. T. H-F. Liedenbaum and J. J. M. Vleggaar; Synth. Metals 85, 1287 (1997).

10. J. Gruner, M. Remners and D. Neher; Adv. Mater. 9, 964 (1997).

11. C. W. Tang and S. A. Vanslyke, Appl. Phys. Lett. 51, 913 (1987).

12. C. W. Tang and S. A. Vanslyke, J. Appl. Phys. 65, 3610 (1989).

13. N. Tesler, G. J. Denton, and R. H. Friend, Nature **382** , 695 (1996)

14. W. Brutting, Stefen Berleb and Anton G. Muckl; Org. Elect. **2**, 1 (2001).

15. E. lebdev, th. Dittrich, V. Petrova-Koch, S. Karg and W. Brutting; Appl. Phys. Lett. **71**, 2686 91997).

16. P. W. Blom, M. J. M. deJong and J. J. M. Vleggaar; Appl. Phys. Lett. 68, 3308 (1996).

17. P. W. M. Blom and M. J. M. deJong; IEEE J. Quant. Elect. 4, 1077 (1998).

18. M. A. Lempert and P. Mark; Current injection in solids, Academic Press, Newyork (1970).

19. R. H. Fowler and L. Nordeim, Proc. R. Soc. London Ser.A 119, 173 (1928).

20. D. Hertel, H. Bassler, V. Scherf and H. H. herhold; J. Chem. Phys. **110**, 9214 (1999).

21. D. M. Pai; J. Chem. Phys. **52**, 2285 (1970).

22. W. D. Gill; J. Appl. Phys. **43**, 5033 (1972).

23. P. W. M. Blom, M. C. J. M. Vissenberg; Phys. Rev. Lett. **80**, 3819 (1998).

24. J. Frenkel; Phys. Rev. **54**, 647 (1938).

25. H. Bassler; Phys. Statics, Solidi B **175**, 15 (1993).

26. S. V. Novikov, D. H. Dunlop, V. M. Kenkre, P. E. Parris and A. V. Vinnikov ; Phys. Rev. Lett. **81**, 4472 (1998).

27. S. V. novikov, and A. V. Vinnikov ; J. Phys. Chem. **99**, 14573 (1995).

28. A. K. Jonscher and A. A. Ansari ; Phylos. Mag. 23, 205 (1971).

29. B. G. Bagley ; Solid State Commu. 8, 345 (1970).

30. P. R. Emtaje ; Phys. Rev. B 3, 2685 (1971).

31. I. Holstein ; Ann. Phys. (N. Y.) 8, 343 (1959).

32. M. D. Tabak, D. M. Pai, and M. E. Scharfe ; J. Non-cryst. Solids 6, 357 (1971).

33. L. B. Schein ; Philos. Mag. B 65, 795 (1992).

34. D. H. Dunlop, P. E. Parris and V. M. Kenkre ; Phys. Rev. Lett. 77, 542 (1996).

35. S. V. Novikov, D. h. Dunlop, V. M. Kenkre, P. E. Perris and A. V. Vonnikov ; Phys. Rev. Lett. 81, 4472 (1998).

36. H. Meyer, D. Haarer, N. Naarman, and H. H. Horhold ; Phys. Rev. B, 52, 2587 (1995).

37. E. Lebdev, Th. Dittrich, Petrova-Koch, S. Karg, and W. Brutting ; Appl. Phys. Lett., 71, 2686 (1997).

38. A. Many, and G. Ratavy ; Phys. Rev., 126, 1980 (1962).

39. E. Pinotti, A. Sassella, A. Borghesi, and R. Tubino ; Synth. Met., 122, 169 (2001).

40. Dario Natali, and Marko Sampietro ; J. Appl. Phys. 92, 5310 (2002).

41. N. F. Mott, and R. W. Gurnay ; Electronic Process in ionic solids Clarendon Oxford, 167 (1948).

42. H. C. F. Martenes, H. B. Brom, and P. W. M. Blom, Phys. Rev. B 60, R8489 (1999).

43. H. C. F. Martenes, J. N. Huiberts and P. W. M. Blom, Appl. Phys. Lett. 77, 1852 (2000).

44. H. Vestweber, R. Sander, A. Greiner, W. Heitz, R.F. Mahrt and H. Bassler ; Synth. Met. 64, 141 (1994).

45. S. Karg, V. Dyakov, M. Meier, W. Reib, and G. Paasch ; Synth. Met. 67, 165 (1994).

46. J. Wang, R. G. Sun, G. Yu, and A. J. Heeger ; Synth. Met. 137, 1009 (2003).

47. C.H. Tan, A. R. Inogo, W. Fann, P. K. Wei, G. Y. Perng, and S. A. Chen, Org. Elect. 3, (2002) 81.

48. J. P. Markham, T. D. Anthopolous, D. W. Samuel, G. J. Richard, P.L. Burn, C. Im, and H. Bassler, App. Phys. Lett. 81 (2002) 3266.

49. R. L. Martin, J. P. Kress, I. H. Campbell, and D. L. Smith, Phy. Rev. B 61 (2000) 15804.

50. M. Gailberger and H. Bassler, Phys. Rev. B 44, 8643 (1991).

51. M. Redecker, D. D. C. Bradliey, M. Inbasekaran, and E. P. Woo ; Appl. Phys. Lett. 73, 1565 (1998).

52. P. W. M. Blom, and M. C. I. M. Vicsenberg ; Phys. Rev. Lett. 80, 3819 91998).

53. E. Lebedev, S.Karg, and W. Brutting ; Appl. Phys. Lett. 71, 2686 (1997).

54. W. Brutting, E. Lebdev, S. Karg, T. Dittrich, V. Petrova-Koch, and M. Schwoerer ; Proc. SPIE 3281, 257 (1998).

55. I. D. Parker, J. Appl. Phys. 75 (1994) 1656.

56. R. H. Friend, R. W. Gymer, A. B. Holmes, R. N. Marks, C. Taliani, D. D. C. Bradley, D. A. Dos Santos, J. L. Bredas, M. Logdlund, and W. R. Salaneck, Nature 397 (1999) 121.

57. L. Bakueva, D. Matheson, S. Musikhin and E. H. Sargent,; Synth. Mat. 126 (2002) 207.

58. G. Rumbles, I.D.W. Samuel, C. J. Collins, P. F. Miller, S. C. Moratti, and A. B. Holmes, Synth. Met. 101 (1999) 159.

59. H. C. F. Martenes, P.W. M. Blom, and H. F. M. Schoo, Phys Rev. B 61 (2000) 7490

60. P. W. M. Blom, H. F. M., and M. Matters, Appl. Phys. Lett. 73 (1998) 3915.

61. P. K. H. Ho, and R. h. Friend, J. Chem. Phys. 116 (2002) 6791.

62. K. Pichler, L. P. Jarett, R. H. Friend, B. Ratier, and A. Moliton, J. App. Phys. 77 (1995) 3523

63. D. J. Pinner, R. H. Friend, and N. Tessler, J. App. Phys. 86 (1999) 5116.

64. C. Adachi, T. Tsatsui and S. Satio, Appl. Phys. Lett. 55, 1489 (1989).